JPET Fast Forward. Published on November 14, 2006 as DOI: 10.1124/jpet.106.110718

JPET#110718

Sphingosine 1-phosphate causes airway hyperreactivity by Rho-mediated myosin phosphatase inactivation

Hiroaki Kume, Naoya Takeda, Tetsuya Oguma,
Satoru Ito, Masashi Kondo, Yasushi Ito,
Kaoru Shimokata

Department of Respiratory Medicine
Nagoya University Graduate School of Medicine
65 Tsrumai-cho, Showa-ku, Nagoya 466-8550, Japan

JPET Fast Forward. Published on November 14, 2006 as DOI: 10.1124/jpet.106.110718
This article has not been copyedited and formatted. The final version may differ from this version.

Running title: Effects of S1P on airway hyperreactivity by MYPT1

Corresponding author:
Hiroaki Kume
Department of Respiratory Medicine
Nagoya University Graduate School of Medicine
65 Tsrumai-cho, Showa-ku, Nagoya 466-8550, Japan
Phone: 81-52-744-2167, FAX: 81-52-744-2176
e-mail: hkume@med.nagoya-u.ac.jp

The number of text page: 30
The number of tables: 0
The number of figures: 6
The number of references: 36
Abstract: 243 words
Introduction: 510 words
Discussion: 1323 words

Abbreviations:
Y-27632, (R)-(+)-trans-N-(4-Pyridyl)-4-(1-aminoethyl)-cyclohexane-carboxamide;
SKF-96365, 1-{β-[3-(4-methoxyphenyl) propoxy]-4-methoxyphenethyl}-1*H*-imidazole hydrochloride

Abstract

In the present study, we investigated whether extracellular sphingosine 1-phosphate (S1P) is involved in airway hyperreactivity in bronchial asthma. The effects of S1P on the response to methacholine was examined in the fura-2 loaded strips of guinea pig tracheal smooth muscle using simultaneous recording of the isometric tension and the ratio of fluorescence intensities at 340 and 380 nm (F_{340}/F_{380}). A 15-min pretreatment with S1P (>100 nM) markedly enhanced methacholine-induced contraction without elevating F_{340}/F_{380}. This effect of S1P was suppressed in the presence of Y-27632, a selective inhibitor of Rho-kinase, in a concentration-dependent manner. Moreover, pretreatment with pertussis toxin caused an inhibition in S1P-induced hyperreactivity to methacholine in a time- and concentration-dependent manner. In contrast, although S1P-induced Ca^{2+} mobilization was attenuated by SKF-96365 and verapamil, the subsequent response to methacholine was unaffected. A 15-min pretreatment with lower concentrations of S1P (<100 nM), which is clinically attainable, did not increase methacholine-induced contraction. However, when the incubation was lengthened to 6 h, S1P (<100 nM) enhanced the subsequent response to methacholine. Next, application of S1P to cultured human bronchial smooth muscle cells increased the proportion of active RhoA (GTP-RhoA), and phosphorylation of myosin phosphatase target subunit 1 (MYPT1). This phosphorylation of MYPT1 was significantly inhibited by application of Y-27632, and by pretreatment with pertussis toxin. Our findings demonstrate that exposure of airway smooth muscle to S1P results in airway hyperreactiviy mediated by Ca^{2+} sensitization via inactivation of myosin phosphatase, which links G_i and RhoA/Rho-kinase processes.

INTRODUCTION

Sphingosine 1-phosphate (S1P), a bioactive lysophospholipid, is generated in the plasma membrane of various cells by sphingolipid metabolism. It is generally considered that S1P is capable of a wide spectrum of biological effects, including cell growth, cell differentiation, cell survival, and cell migration (Spiegel and Milstien, 2000). Recent clinical trials have demonstrated that the level of S1P is dramatically elevated in bronchoalveolar lavage (BAL) fluid from patients with asthma following allergen challenges (Ammit et al., 2001; Jolly et al., 2001). In vitro, FcεRI cross-linking, which elicits the IgE-mediated allergic reaction, activates sphingosine kinase, resulting in the conversion of shingosine to S1P (Jolly et al., 2004). S1P is released from mast cells, and plays an important role not only in regulating mast cell functions but also eosinophil chemotaxis (Rosenfeldt et al., 2003; Roviezzo et al., 2004). Moreover, extracellular S1P modulates the production of proinflammatory cytokines and cell proliferation. Therefore, S1P may act as a lipid mediator in the pathophysiology of bronchial asthma.

External application of S1P to smooth muscle in a various tissues causes contraction with an increase in the concentrations of intracellular Ca^{2+} ($[Ca^{2+}]_i$) (Watterson et al., 2005). The Ca^{2+} mobilization induced by S1P are mediated by Ca^{2+} influx pass through voltage-dependent L-type Ca^{2+} (VDC) channels and store operated Ca^{2+} entry (Rosenfeldt et al., 2003; Bischoff et al., 2000; Ghosh et al., 1990). On the other hand, Rho, a small GTPase, and Rho-kinase, a specific effecter of Rho, are involved in the post-receptor signal transduction pathways of S1P (Rosenfeldt et al., 2003; Coussiun et al., 2002; Zhou and Murthy, 2004; Salomone et al., 2003). However, in smooth muscle contraction induced by S1P, the role of Ca^{2+} sensitization that relates

JPET Fast Forward. Published on November 14, 2006 as DOI: 10.1124/jpet.106.110718
This article has not been copyedited and formatted. The final version may differ from this version.

to Rho/Rho-kinase pathways remains unclear. Extracellular S1P acts as a ligand for a family of specific G-protein coupled receptors ($S1P_{1-5}$), which are coupled to a variety of G proteins that are linked, in turn, to downstream signaling pathways (Payne et al., 2002; Siehler and Manning, 2002). In the respiratory system including airway smooth muscle (ASM), it is generally considered that $S1P_2$ may play an important physiological role (Rosenfeldt et al., 2003). Previous studies in cultured human ASM cells using mechanically loaded collagen matrix have shown that S1P causes contraction by activating L-type voltage-dependent Ca^{2+} (VOC) channels (Rosenfeldt et al., 2003). Moreover, the S1P-induced contraction in ASM cells is mediated by pertussis toxin (PTX)-insensitive processes (Rosenfoldt et al., 2003). However, it has been proposed that G_i may participate S1P-induced contraction of smooth muscle in other tissues (Zhol and Murthy, 2004; Salmone et al., 2003; Bischoff et al., 2000). Little is currently known about S1P action in ASM although it could act as a mediator of the interaction between inflammatory cells and ASM in bronchial asthma.

This study was designed to determine whether extracellular S1P is involved in airway hyperreactivity, which is implicated in the pathophysiology of bronchial asthma. To identify the molecular mechanisms of regulating ASM contractility following continuous exposure to S1P, we focused on the role of Ca^{2+} mobilization and Ca^{2+} sensitization in the post-receptor signal transduction pathways activated by S1P.

METHODS

Tissue Preparation and Solution

Male Hartley guinea pigs (300-350 g) were killed by injection of overdose of anesthetics (150 mg/kg pentobarbital, i.p.) and tracheas were excised. The tracheal rings were opened by cutting longitudinally at the cartilaginous region, and the epithelium was dissected out. The normal bathing solution was composed of (in mM): NaCl 137, $KHCO_3$ 5.9, $CaCl_2$ 2.4, $MgCl_2$ 1.2, and glucose 11.8, bubbled with a mixture of 99% O_2 and 1% CO_2 (pH 7.4). The organ bath was filled with the bathing solution at a constant flow of 3 ml/min, and the temperature of the organ bath was maintained at 37 °C. All animal procedures were approved by The Animal Care and Use Committee, Nagoya University Graduate School of Medicine.

Isometric Tension Recording and Measurement of Fura-2 Fluorescence

Isometric tension and fura-2 fluorescence were measured essentially as described previously (Kume and Takagi, 1997; Kume et al., 2001). Muscle strips containing four cartilaginous rings, one for isometric tension recording and three for measurement of $[Ca^{2+}]_i$ were prepared. Muscle strips were treated with 10 μM acetoxymethyl ester of fura-2 for 4 h at room temperature (22-24 °C). The non-cytotoxic detergent, pluronic F-127 (0.01% wt/vol), was added to increase the solubility of fura-2. After the loading, the chamber was filled with the normal bating solution at 37 °C for 50 min to wash out the extracellular fura-2 prior to the measurements. Isometric tension and the fura-2 fluorescence of the muscle strips were measured simultaneously, using a displacement transducer and a spectrofluorometer (CAF-110; Japan Spectroscopic, Tokyo, Japan). The intensities of fluorescence due to

excitation at 340 nm (F_{340}) and 380 nm (F_{380}) were measured after background subtraction. The absolute amount of $[Ca^{2+}]_i$ was not calculated because the dissociation constant of fura-2 for Ca^{2+} in smooth muscle cytoplasm is different from that obtained *in vitro* (Konishi et al., 1988). Therefore, the ratio of F_{340} to F_{380} (F_{340}/F_{380}) was used as a relative indicator of $[Ca^{2+}]_i$. Muscle tension and F_{340}/F_{380} in the resting state were taken as 0%, and the values of percent contraction and percent F_{340}/F_{380} were expressed by taking response to 1 μM methacholine (MCh) or 10 μM histamine at each experimental condition as 100%. Time-matched control tissues were treated similarly to the test tissues but exposed continuously to the normal bathing solution instead of S1P, and PTX. The resting tone was abolished by addition to 2 μM indomethacin throughout the experiments.

Cell Culture

Primary cultures of normal human bronchial smooth muscle (BSM) cells from multiple donors were obtained from Cambrex (Walkersville, MD, USA.). The cells were maintained in culture medium, containing 5% fetal bovine serum (FBS), human recombinant EGF (1 ng/ml), insulin (10 mg/ml), human recombinant fibroblast growth factor (2 ng/ml), gentamicin (50 mg/ml) and amphotericin B (0.05 mg/ml) (SmGM-2 BulletKit, Cambrex) in an atmosphere of 5% CO_2 and 95% air at 37°C. Cells at the fifth - seventh passage were used for the experiments.

RhoA Activation Assay

The amount of activated Rho (GTP-Rho) was determined using a Rho activation assay kit (Upstate Biotechnology, Inc., Lake Placid, NY, USA). The human BSM cells were

grown to confluence and then placed in serum-free medium (DMEM/F-12; Invitrogen, Carlsbad, CA, USA) containing antibiotics-antimycotic (penicillin 100 units/ml streptomycin 100 μl/ml, amphotericin B 250 ng/ml; Invitrogen) for 24 h. After stimulation by S1P, the cells were washed with ice-cold phosphate-buffered saline (PBS). Cellular lysates were prepared according to the manufacturer's instructions.

Phosphorylation of Myosin-binding Subunit (MBS)

Phosphorylation of MBS was evaluated with specific antibodies for myosin phosphatase target subunit 1 (MYPT1). The human BSM cells were grown to confluence and then placed in serum-free medium for 24 h. After exposure to agents, the BSM cells were washed with ice-cold PBS. Whole-cell lysates were prepared by treating the cells with lysis buffer (50 mM Tris-HCl, pH 6.8, 10% glycerol, 2% sodium dodecylsulfate, 5% 2-mercaptoethanol).

Western Blot

Protein contents of cellular lysates were measured using a Bio-Rad protein assay reagent kit (Bio-Rad, Hercules, CA, U.S.A.) according to the manufacturer's instructions. Equal amounts of lysates, adjusted to protein content, were resolved by SDS-PAGE using a 4-20% linear gradient running gel. Proteins were transferred to a nitrocellulose membrane and the membrane was incubated at room temperature in PBS containing 0.2% Tween 20 (PBS-T buffer) for 1 h. Immunoblotting was performed using antibodies against RhoA, MYPT1 (Santa Cruz, Santa Cruz, CA, U.S.A.), and anti-phospho-MYPT1 (Thr^{850}) (Upstate Biotechnology, Inc.). Immunodetection was accomplished using a sheep anti-mouse secondary antibody or donkey anti-rabbit

secondary antibody and the enhanced chemiluminescence kit (Amersham Biosciences, Piscataway, NJ, U.S.A.). The intensity was quantified using Scion image software (Scion Image, Frederick, MD, USA).

Experimental Protocols

To examine the effects of S1P on ASM, the fura-2 loaded tissues of guinea pig tracheal smooth muscle were treated with S1P for 15 min. Before and after application of S1P, the strips were washed out for 10 min with the normal bathing solution. To examine the effects of S1P on airway hyperreactivity, the contraction and F_{340}/F_{380} in response to 1 μM MCh and 10 μM histamine were measured before and after exposure to S1P. To determine the involvement of Ca^{2+} mobilization by S1P in the pathogenesis of airway hyperreactivity, the tension and F_{340}/F_{380} in response to MCh were examined before and after exposure to S1P in the absence and presence of Ca^{2+} channel blockers such as SKF-96365, a non-selective inhibitor of Ca^{2+} channels, and verapamil, a selective inhibitor of voltage-dependent Ca^{2+} channels. To determine the involvement of Ca^{2+} sensitization by S1P in these mechanisms, response to MCh was similarly examined in the absence and presence of Y-27632, a selective inhibitor of Rho-kinase, PD98059, an inhibitor of mitogen-activated protein kinase (MEK), and bisindolylmaleimide, an inhibitor of protein kinase C. When the period for incubation with S1P (<100 nM) was lengthened to 6h, the strips were not loaded with the fura-2. To determine the involvement of G_i, the inhibitory G protein of adenylyl cyclase, in the augmentation of MCh-induced contraction by S1P, the strips were pretreated with ~ 1 μg/ml PTX for ~ 6h, and then the response to MCh was examined after exposure to S1P. To determine relationships between S1P and RhoA, after treating the human BSM cells with ~ 3 μM

S1P for 15 min, GTP-RhoA was measured using the RhoA activation assay. Moreover, to confirm the effects of S1P on RhoA, phosphorylation of MYPT1, a direct target substrate of Rho-kinase, was measured in the human BSM cells using Western blots. To determine the involvement of Rho-kinase and extracellular signal-regulated kinase (ERK) in the stimulation of MYPT1 phosphorylation by S1P, the cells were treated with Y-27632 and PD 98059, respectively, 30 min prior to stimulation by S1P. To determine the involvement of G_i in this phosphorylation, the cells were treated with 100 ng/ml PTX for 4h prior to stimulation with S1P.

Agents

MCh, indomethcin, PTX, varapamil, bisindolylmaleimide, histamine and pluronic F-127 were obtained from Sigma (St. Louis, MO, U. S. A.). S1P was obtained from BIOMOL (Plymouth Meeting, PA, U.S.A). Y-27632 was obtained from Wako (Osaka, Japan). SKF96365 and PD98059 were obtained from Calbiochem (La Jolla, CA, U.S.A.). Fura-2/AM was obtained from Dojin Laboratories (Kumamoto, Japan).

Statistics

All data was expressed as means ± S. D., and response to an agent under each experimental condition was described as the percent of the control condition. Values of concentration of agents that produces a 50% response (EC_{50}) of contraction by 1 μM MCh were determined using regression analysis applied to the linear portion of each concentration-response curve. Statistical significance was assessed by Student's t-test or repeated-measures ANOVA, followed by Bonferroni post hoc test. A probability below 0.05 ($p < 0.05$) was considered to be a significant difference.

JPET Fast Forward. Published on November 14, 2006 as DOI: 10.1124/jpet.106.110718
This article has not been copyedited and formatted. The final version may differ from this version.

RESULTS

Role of Ca^{2+} sensitization in the induction of airway hyperreactivity by S1P

In fura-2 loaded tissues, S1P (0.03 - 10 μM) caused a concentration-dependent generation of force with an increase in F_{340}/F_{380}. The concentration-response curve for F_{340}/F_{380} induced by S1P was upper area than that curve for tension induced by S1P (Figure 1B). The value of percent contraction in response to 3 μM S1P was 52.4 ± 10.5%, whereas the value of percent F_{340}/F_{380} in response to an equi-molar of S1P was 95.1 ± 3.1% (n = 10, $p < 0.01$, Figure 1B). A 15-min exposure to 3 μM S1P markedly enhanced MCh-induced contraction without affecting F_{340}/F_{380} (Figure 1A). As shown in Figure 1C, pretreatment with S1P (0.03 - 3 μM) caused an increase in the contraction induced by MCh in a concentration-dependent manner. The values of percent contraction for MCh after treatment without and with 3 μM S1P were 99.6 ± 9.8 (n = 10) and 138.5 ± 9.2% (n = 10, $p < 0.01$), respectively. In contrast, the values of percent F_{340}/F_{380} for MCh were 96.8 ± 9.8 (n = 10) and 100.8 ± 9.4% (n = 10, not significant), respectively. Contraction induced by 10 μM histamine was also augmented without elevating F_{340}/F_{380} after exposure to equi-molar S1P for an equivalent time (Figure 1D). The values of percent contraction and percent F_{340}/F_{380} after exposure to 3 μM S1P were 129.8 ± 8.4 ($p < 0.01$) and 98.6 ± 7.8 (not significant, respectively (n = 8). Next, MCh was applied cumulatively to the fura-2 unloaded tissues between 0.001 and 10 μM before and after incubation with S1P (0.003 - 0.03 μM) for 6 h. Under this experimental condition, the concentration-response curves for MCh were markedly shifted to the left in a concentration-dependent manner (Figure 1E). The values of

JPET Fast Forward. Published on November 14, 2006 as DOI: 10.1124/jpet.106.110718
This article has not been copyedited and formatted. The final version may differ from this version.

EC_{50} for the curves after treatment without and with 0.03 μM S1P were 0.59 ± 0.18 (n = 12) and 0.05 ± 0.02 μM (n = 12, P < 0.01), respectively.

Involvement of Ca^{2+} sensitization by Rho-kinase in the induction of airway hyperreactivity by S1P

In the presence of 1 μM Y-27632, 3 μM S1P-induced contraction was markedly attenuated without reducing F_{340}/F_{380} (Figure 2A). After exposure to 3 μM S1P with 1 μM Y-27632, both contraction and F_{340}/F_{380} induced by 1 μM MCh was not augmented (Figure 2A). Application of Y-27632 (0.01 - 1.0 μM) caused an inhibition in the enhancement of MCh-induced contraction by S1P in a concentration-dependent manner. The value of percent contraction for MCh after exposure to 3 μM S1P with 1 μM Y-27632 was decreased to 100.4 ± 9.4% (n = 8, p < 0.01) (Figure 2B). In contrast, the values of percent for F_{340}/F_{380} for MCh were unaffected (Figure 2B). After exposure of the tissues to Y-27632 without S1P, MCh-induced contraction was not reduced (data not shown). MCh (0.001 - 10 μM) was cumulatively applied to the fura-2 unloaded tissues before and after exposure to 0.03 μM S1P with Y-27632 (0.1 - 1.0 μM) for 6h. The concentration-response curve for MCh after exposure to S1P was shifted to the right by addition of Y-27632 in a concentration-dependent manner. The values for EC_{50} for the curves for MCh after exposure to 0.03 μM S1P in the absence and presence of 1.0 μM Y-27632 were 0.06 ± 0.04 (n = 10) and 0.41 ± 0.16 μM (n = 10, p < 0.01), respectively (Figure 2C).

Next, in the presence of 30 μM PD98059, response to MCh was examined before and after exposure to 3 μM S1P for 15 min. However, under this experimental

JPET Fast Forward. Published on November 14, 2006 as DOI: 10.1124/jpet.106.110718
This article has not been copyedited and formatted. The final version may differ from this version.

condition, the contraction induced by 1 μM MCh following exposure to S1P was increased without an elevation in F_{340}/F_{380}, similar to the result shown in Figure 1A. The values of percent contraction and percent F_{340}/F_{380} for MCh were 134.9 ± 12.4 (not significant) and 105.2 ± 9.2% (not significant), respectively (n = 6, Figure 2D). In the presence of 10 μM bisindoylmaleimide, MCh-induced contraction after exposure to S1P was also augmented without a change in F_{340}/F_{380}. The values of percent contraction and percent F_{340}/F_{380} for MCh were 131.2 ± 14.4 (not significant) and 102.2 ± 9.7% (not significant), respectively (n = 6, Figure 2D).

Ca^{2+} mobilization by is not involved in the induction of airway hyperreactivity by S1P

100 μM SKF-96365 resulted in a marked suppression of both tension and F_{340}/F_{380} induced by 3 μM S1P (Figure 3A). However, after exposure to S1P with SFK-96365, 1 μM MCh-induced contraction was markedly increased without elevating F_{340}/F_{380}, similar to the result shown in Figure 1A. The values of percent contraction and percent F_{340}/F_{380} for MCh after exposure to S1P with SKF-96365 were 129.7 ± 12.9 (n = 6, not significant) and 96.3 ± 9.8% (n = 6, not significant), respectively (Figure 3B). 10 μM verapamil caused a modest inhibition in the augmented tension and F_{340}/F_{380} by equi-molar S1P (data not shown). Moreover, after exposure to S1P in the presence of verapamil, 1 μM MCh-induced contraction was markedly increased independent of F_{340}/F_{380}, similar to the results shown in Figure 1A. The values of percent contraction and percent F_{340}/F_{380} for MCh after exposure to S1P in the presence of verapamil were 134.1 ± 12.1 (n = 6, not significant) and 102.4 ± 13.1% (n = 6, not significant), respectively (Figure 3B).

JPET Fast Forward. Published on November 14, 2006 as DOI: 10.1124/jpet.106.110718
This article has not been copyedited and formatted. The final version may differ from this version.

Involvement of G_i in the induction of airway hyperreactivity induced by S1P

Pretreatment of the fura-2 unloaded tissues with PTX 1 μg/ml for ~ 6 h caused a marked attenuation of the augmented response to 1 μM MCh after exposure to 3 μM S1P in a time-dependent manner (Figures 4A, and 4B). The values of percent contraction for MCh after exposure to S1P, followed by treatment without and with PTX for 6 h were 134.6 ± 12.8 (n = 8), and 102.5 ± 8.6% (n = 8, P < 0.01), respectively (Figure 4B). MCh (0.001 - 10 μM) was cumulatively applied to the tissues before and after incubation with 0.1 and 1.0 μg/ml PTX in the presence of 0.03 μM S1P for 6h. The concentration-response curves for MCh after exposure to S1P with PTX were shifted to the right in a concentration-dependent manner (Figure 4C). The values of EC_{50} for the curves for MCh after exposure to S1P without and with 1.0 μg/ml PTX for 6h were 0.08 ± 0.05 (n = 8), and 0.48 ± 0.18 μM (n = 8, p < 0.01), respectively (Figure 4C).

Effects of S1P on RhoA activation in ASM cells

After cultured human BSM cells were exposed for 15 min to serum-free medium in the absence (control) and presence of 3 μM S1P, relative proportion of RhoA-GTP to total RhoA (RhoA-GTP/total RhoA) was measured using the Rhotekin binding domain assay. The value of RhoA-GTP/total RhoA was increased to 2.3 ± 0.2 fold (n = 4) by application of 3 μM S1P, compared with the control (p < 0.01, Figure 5).

Effects of S1P on the phosphorylation of MYPT1 in ASM cells

Application of S1P (0.3 - 3 μM) for 15 min caused a concentration-dependent increase in MYPT1 (Thr^{850}) phosphorylation in human BSM cells (Figure 6A). An

increase in phosphorylation of MYPT1 (Thr^{850}) by 3 μM S1P was significantly inhibited in the presence of Y-27632 (0.1 - 1.0 μM) in a concentration-dependent manner (Figure 6B). In contrast, under the experimental condition of exposure to S1P in the presence of 30 μM PD98059, phosphorylation of MYPT1 (Thr^{850}) by S1P was not affected (Figure 6C). However, when the human BSM cells were pretreatment with 0.1 μg/ml PTX for 4 h, the effect of S1P on phosphorylation of MYPT1 (Thr^{850}) was markedly suppressed (Figure 6C).

JPET Fast Forward. Published on November 14, 2006 as DOI: 10.1124/jpet.106.110718
This article has not been copyedited and formatted. The final version may differ from this version.

Discussion

The principal observations in this study are as follows: 1) S1P directly suppresses myosin phosphatase (MP) activity by the phosphorylation of MYPT1, which is a direct target substrate of Rho-kinase: 2) Pretreatment with S1P leads to an increase in MCh-induced contraction mediated by Ca^{2+} sensitization via the MP inactivation processes: and 3) PTX-sensitive processes are involved in the functional effects of S1P on the induction of airway hyperreactivity.

The contractile effect of S1P on ASM has not been previously investigated in tissue samples, although studies in vascular smooth muscle have demonstrated that S1P induces contraction at concentrations above 100 nM (Bischoff et al., 2000; Salomone et al., 2003; Tosaka et al., 2001), similar results were observed in ASM (Figure 1B). Although the level of S1P in BAL fluid is elevated by an antigen challenge in patients with asthma, the concentration is less than 100 nM (Ammit et al., 2001; Jolly et al. 2001). Hence, extracellular S1P may not have a direct role in bronchoconstriction associated with bronchial asthma. Pretreatment with concentrations of S1P below 100 nM for 15 min also did not enhance subsequent responses to MCh or histamine (Figures 1A, 1C and 1D). However, when the period of incubation with S1P was extended to 6 h, lower concentrations of S1P (3 - 30 nM), which are similar to the level attained in BAL fluid after an antigen challenge, caused a marked enhancement of the response to MCh (Figure 1E). These results in isolated guinea pig ASM tissues were also observed in isolated human ASM tissues effects (data not shown). Therefore, although whether S1P is related to airway hyperreactivity in patients with asthma remains unknown, our results suggest that extracellular S1P, which is released from inflammatory cells, can lead to airway hyperreactivity clinically.

JPET Fast Forward. Published on November 14, 2006 as DOI: 10.1124/jpet.106.110718
This article has not been copyedited and formatted. The final version may differ from this version.

As shown in Figures 1B, and 3A, S1P is less potent in enhancing the sensitivity to intracellular Ca^{2+} than MCh, and that Ca^{2+} influx passing through Ca^{2+} channels non-selectively plays a functional important role in S1P-induced contraction. S1P has modest effects on verapamil-sensitive Ca^{2+} channels. In addition, similar to our observations, previous patch clamp studies have shown that in endothelial cells, S1P activates non-selective cation channels (Muraki and Imaizumi, 2001). Furthermore, our results indicates that Ca^{2+} sensitization mediated by Rho-kinase is involved in the functional effects of S1P on ASM (Figure 2A). External application of S1P augments RhoA activity and the phosphorylation of MYPT1 (Figures 5 and 6), demonstrating that a loss of MP activity via activation of the RhoA/Rho-kinase processes play an important role in the action of S1P in ASM. Although a few reports have shown that S1P phosphorylates myosin light chain in smooth muscle containing airways (Rosenfeldt et al., 2003; Zhou and Murthy, 2004), the main action of Rho-kinase in Ca^{2+} sensitization appears to be the inhibition in MP activity due to phosphorylation of MBS (Kimura et al., 1996; Matsui et al., 1996; Fukata et al., 2001). As shown in this study, Rho-kinase acts on MYPT1 in ASM, which is similar to findings in vascular smooth muscle (Velasco et al., 2002; Liu et al., 2004; Wilson et al., 2005). Therefore, phosphorylation of myosin light chain is an indirect response to S1P as a result of inhibition in MP activity by Rho-kinase.

We also examined the involvement of Ca^{2+} mobilization and Ca^{2+} sensitization in the induction of airway hyperreactivity after exposure to S1P. As shown in Figures 1A and 1C, Ca^{2+} sensitization is involved in an increase in MCh-induced contraction after exposure to S1P. When S1P-induced contraction was suppressed in the presence of Y-27632 independent of $[Ca^{2+}]_i$, the augmented response

to MCh after exposure to S1P was abolished in a concentration-dependent manner (Figures 2A, and 2B). Moreover, Y-27632 also suppressed the ability of an extended treatment with the clinical levels of S1P to enhance the effects of MCh (Figure 2C). Therefore, Ca^{2+} sensitization via Rho-kinase-dependent inactivation of MP participates in the ability of S1P to induce airway hyperreactivity. In contrast, even though both tension and $[Ca^{2+}]_i$ by S1P was suppressed in the presence of SKF-96365 and verapamil, the ability of S1P to enhance MCh-induced contraction was unaffected by these Ca^{2+} antagonists (Figures 3A and 3B). These results provide further support the idea that Ca^{2+} sensitization but not Ca^{2+} mobilization is involved in the effect of S1P on the induction of airway hyperreactivity in ASM. However, as shown in Figure 2D, ERK and protein kinase C do not appear to be involved in the Ca^{2+} sensitization by S1P (Shirao et al., 2002).

Next, we sought to determine the involvement of the receptor and post-receptor signal transduction pathways in the induction of airway hyperreactivity after treatment with S1P. As shown in figures 4A, 4B and 4C, preincubation with PTX causes an inhibition in the enhancement of MCh-induced contraction by S1P in time- and concentration-dependent manners. Since exposure to PTX causes a functional uncoupling of G_i, the inhibitory heterotrimeric G protein of adenyly cyclase, from its associated receptor via the ADP ribosylation, G_i may mediate the ability of S1P to cause hyperreactivity to MCh. A previous report has indicated that MCh-induced contraction in ASM is partly attenuated after exposure to PTX (Kume et al., 1995). Although the inhibitory effects of PTX on the S1P-induced hyperreactivity to MCh may be due to muscarinic inhibition by PTX, incubation with PTX directly suppressed the phosphorylation of MYPT1 by S1P (Figure 6C). Moreover, in ASM the

hyperresponsiveness to histamine were similarly observed by pretreatment with S1P (Figure 1D). These results indicate that an inhibition in the muscarinic hyperreactivity by S1P is due to a PTX-sensitive pathway that alters the action of S1P rather than a direct effect of the PTX-sensitive pathway on muscarinic action. In endothelial cells, activation of non-selective cation channels by S1P is also suppressed by pretreatment with PTX (Muraki and Imaizumi, 2001). Although it remains unclear whether G_i is involved in the effect of S1P on ASM, our results demonstrate that G_i is related to S1P-induced hyperreactivity to MCh via activation of MP. In smooth muscle other than ASM, external application of S1P augmented both force generation and $[Ca^{2+}]_i$ via a PTX-sensitive process (Bischoff et al., 2000; Salmone et al., 2003; Zhou and Murthy, 2004). Moreover, in non smooth muscle, the effect of S1P is antagonized by PTX (Liu et al., 2001; Rouch et al., 2006). As shown in Figure 6, the phosphorylation of MYPT1 was markedly attenuated after exposure to 0.1 μg/ml PTX for 4 h. In ASM cells, the inhibitory effects of MCh on Ca^{2+}-activated K^+ channel activity is eliminated by a 4-h pretreament with PTX (Kume and Kotlikoff, 1991; Kume et al., 1992). In ASM tissues, in contrast, more than 4 h are needed for the maximun effect of PTX.

It is generally considered that $S1P_3$ receptors are coupled to G_i (Siehler and Manning, 2002; Ancellin and Hla, 1999; Hla et al., 2001), and that it enhances Rho activity (Paik et al., 2001) and Ca^{2+} influx (Ishii et al., 2002). Suramine is a non selective antagonist of $S1P_3$, however, this agent is also used as an inhibitor of S1P (Ancellin and Hla, 1999). In the presence of suramine, the enhancement of MCh-induced contraction by pretreatment with S1P was markedly attenuated in a concentration-dependent manner (data not shown), suggesting that $S1P_3$ is involved in the S1P-induced hyperresposiveness to MCh in ASM. Although the S1P receptor

subtype and the post-receptor pathway have not be fully elucidated yet in this study, loss of MP activity by the relationship between $S1P_3/G_i$ and Rho/Rho-kinase may play a fundamentally functional role in the induction of hyprereactivity to MCh by S1P in ASM.

In conclusion, pretreatment of ASM with the clinical level of S1P leads to an enhancement of contractility of ASM due to Ca^{2+} sensitization via Rho-mediated MP inactivation. Although clinical relevance of these results remainsl unknown, our observation may provide the evidence that S1P acts as a lipid mediator, and that extracellular S1P causes airway hyperreactivity implicated in the pathophysiology of bronchial asthma.

Acknowledgements:

We would like to thank Professor Kozo Kaibuchi (Department of Cell Pharmacology, Nagoya University Graduate School of Medicine) for helpful comments.

References

Ammit AJ, Hastie AT, Edsall LC, Hoffman RK, Amrani Y, Krymskaya VP, Kane SA, Peters SP, Penn RB, Spiegel S, Panettieri Jr RA (2001) Shingosine 1-phosphate modulates human airway smooth muscle cell function that promote inflammation and airway remodeling in asthma. FASEB J 15: 1212-1214.

Ancellin N, Hla T (1999) Dofferential pharmacological properties and signal transduction of the sphingosine 1-phosphate receptors EDG-1, DEG-3, and EDG-5. J Biol Chem 274: 18997-19002.

Bischoff A, Czyborra P, Fetscher C, Meyer zu Heringdorf D, Jacobs KH, Michel MC (2000) Sphingosine 1-phosphate and sphingosylphosphorylcholine constrict renal and mesenteric microvessels in vitro. Br J Pharmacol 130: 1871-1877.

Bischoff A, Czyborra P, zu Heringdorf M, Jacobs KH, Michel MC (2000) Sphingosine 1-phosphate reduces rat renal and mesenteric blood flow in vivo in a pertussis toxin-sensitive manner. Br J Pharmacol 130: 1878-1883.

Coussiun F, Scott RH, Wise A, Nixon GF (2002) Comparison of sphingosine 1-phosphate-induced intracellular signaling pathways in vascular smooth muscles. Differential role in vasoconstriction. Circ Res 91: 151-157.

Fukata Y, Amano M, Kaibuchi K (2001) Rho-Rho-kinase pathway in smooth muscle contraction and cytoskeletal reorganization of non-muscle cells. Trends Pharmacol Sci 22: 32-39.

Ghosh TK, Bian J, Gill DL (1990) Intracellular calcium release-mediated by sphingosine derivatives generated in cells. Science 248: 1653-1656.

Hla T, Lee MJ, Ancellin N, Paik JH, Kluk MJ (2001) Lysophospholipids-receptor

revelations. Science 294: 1875-1878.

Ishii I, Ye X, Friedman B, Kawamura S, Contos JJA, Kingsburry MA, Yang AH, Zhang G, Brown JH, Chun J (2002) Marked perinatal lethality and cellular signaling deficit in mice null for the two sphingosine 1-phosphate (S1P) receptors, S1P2/LP_{B2}/EDG-5 and S1P3/LP_{B3}/EDG-3. J Biol Chem 277: 25152-25159.

Jolly PS, Rosenfeldt HM, Milstien S, Spiegel S (2001) The role of sphingosine 1-phosphate in asthma. Mol Immunol 38: 1239-1245.

Jolly PS, Bektas M, Olivera A, Gonzalez-Espinosa C, Proia RL, Rivera J, Milstien S, Spiegel S (2004) Transactivation of sphingosine 1-phosphate receptors by FceRI triggering is required for normal mast cell degranulation and chemotaxis. J Exp Med 199: 959-970.

Kimura K, Ito M, Amano M, Chihara K, Fukata Y, Nakafuku M, Yamamori B, Feng J, Nakano T, Okawa K, Iwamatsu A, Kaibuchi K (1996) Regulation of myosin phosphatase by Rho and Rho-associated kinase (Rho-kinase). Science 273: 245-248.

Konishi M, Olson A, Hollingworth S, Baylor M (1988) Myoplasmic binding of fura-2 investigated by steady-state fluorescence and absorbance measurements. Biophys J 54: 1089-1104.

Kume H, Kotlikoff MI (1991) Muscarinic inhibition of single K_{Ca} channels in smooth muscle by a pertussis-sensitive G protein. Am J Physiol Cell Physiol 261: C1204-1209.

Kume H, Graziano MP, Kotlikoff MI (1992) Stimulatory and inhibitory regulation of calcium-activated potassium channels by guanine nucleotide-binding proteins. Proc Natl Acd Sci USA 89: 11051-11055.

Kume H, Mikawa K, Takagi K, Kotlikoff MI (1995) Role of G proteins and K_{Ca} channels in the muscarinic and β-adrenergic regulation of airway smooth muscle. Am J Physiol 268: L221-229.

Kume H, Takagi K (1997) Inhibitory effects of G_s desensitization of β-adrenergic receptors in tracheal smooth muscle. Am J Physiol 273: L556-564.

Kume H, Ito S, Ito Y, Yamaki K (2001) Role of lysophosphatidylcholine in the desensitization of β-adrenergic receptors by Ca^{2+} sensitization. Am J Respir Cell Mol Biol 25: 291-298.

Liu F, Verin AD, Wang P, Day R, Wersto RP, Chrest FJ, English DK, and Garcia GN (2001) Differential regulation of sphingosine-1-phosphate- and VEGF-induced endothelial cell chemotaxis. Involvement of $G_{i\alpha 2}$-linked Rho kinase activity. Am J Respir Cell Mol Biol 24: 711-719.

Liu Y, Suzuki YJ, Day RM, Fanburg BL (2004) Rho kinase-induced nuclear translocation of ERK1/ERK2 in smooth muscle cell mitogenesis caused by serotonin. Circ Res 95: 579-586.

Matsui T, Amano M, Yamamoto T, Chihara K, Nakafuku M, Ito M, Nakano T, Okawa K, Iwamatsu A, Kaibuchi K (1996) Rho-associated kinase, a novel serine/threonine kinase, as a putative target for small GTP binding protein Rho. EMBO J 15: 2208-2216.

Muraki K, and Imaizumi Y (2001) A novel function of sphingosine-1-phosphate to activate a non-selective cation channel in human endothelial cells. J Physiol 537: 431-441.

Paik JH, Chae S, Lee MJ, Thangada S, Hla T (2001) Sphingosine 1-phosphate-induced endothelial cell migration requires the expression of EDG-1

and EDG-3 receptors and Rho-dependent activation of $\alpha_v\beta_3$- and β_1-containing integrins. J Biol Chem 276: 11830-11837.

Payne SG, Milstien S, Spiegel S (2002) Sphingosine-1-phosphate: dual messenger functions. FEBS Lett 531, 54-57.

Rosenfeldt HM, Amrani Y, Watterson KR, Murthy KS, Panettieri Jr RA, Spiegel S (2003) Sphingosine 1-phosphate stimulates contraction of human airway smooth muscle cells. FASEB J 17: 1789-1799.

Rouach N, Pebay A, Meme W, Cordier J, Ezan P, Etienne E, Giaume C, and Tence M (2006) S1P inhibits gap junction in astrocytes: involvement of G_i and Rho GTPase/ROCK. Eur J Neurosci 23: 1453-1464.

Roviezzo F, Del Galdo F, Abbate G, Bucci M, D'Agostino B, Antunes E, De Dominicis G, Parente L, Rossi F, Grino G, De Palma R (2004) Human eosinophil chemotaxis and selective in vivo recruitment by sphingosine 1-phosphate. Proc Natl Acad Sci USA 101: 11170-11175.

Salomone S, Yoshimura S, Reuter U, Foley M, Thomas SS, Moskowitz MA, Waeber C (2003) S1P3 receptors mediate the potent constriction of cerebral arteries by sphingosine-1-phosphate. Eur J Pharmacol 469: 125-134.

Shirao S, Kashiwagi S, Sato M, Miwa S, Nakao F, Kurokawa T, Todoroki-Ikeda N, Mogami K, Mizukami Y, Kuriyama S, Haze K, Suzuki M, Kobayashi S (2002) Shingosylphosphorylcholine is a novel messenger for Rho-kinase-mediated Ca^{2+} sensitization in the bovine cerebral artery. Unimportant role for protein kinase C. Circ Res 91: 112-119.

Siehler S, Manning DR (2002) Pathways of transduction engaged by sphingosine 1-phosphate through G protein-coupled receptors. Biochem Biophys Acta 1582:

94-99.

Spiegel S, Milstien S (2000) Sphingosine 1-phosphate: signal inside and outside. FEBS Lett 476: 55-57.

Tosaka M, Okajima F, Hashiba Y, Saito N, Nagano T, Watanabe T, Kimura T, Sasaki T (2001) Sphingosine 1-phosphate contracts canine basilar arteries in vitro and in vivo: possible role in pathogenesis of cerebral vasospasm. Stroke 32: 2913-2919.

Valasco G, Armstrong C, Morrice N, Frame S, and Cohen P (2002) Phosphorylatiion of the regulatory subunit of smooth muscle protein phosphatase 1M at Thr850 induces its dissociation from myosin. FEBS Lett 527: 101-104.

Watterson KR, Ratz PH, Spiegel S (2005) The role of sphingosine-1-phosphate in smooth muscle contraction. Cell Signal 17: 289-298.

Wilson DP, Susnjar M, Kiss E, Sutherland C, and Walsh MP (2005) Thromboxane A2-induced contractiionof rat caudal arterial smooth muscle involves activation of Ca^{2+} entry and Ca^{2+} sensitization: Rho-associated kinase-mediated phosphorylation of MYPT1 at Thr-855, but not Thr-697. Biochem J 389: 763-774.

Zhou H, Murthy KS (2004) Distinctive G protein-dependent signaling in smooth muscle by sphingosine 1-phosphate receptors S1P1 and S1P2. Am J Physiol Cell Physiol 286: C1130-1138.

Footnotes:

This work is supported by Grants-in-Aid from the Ministry of Education, Science, Sports, and Culture of Japan (Kume H, #17590785), and (Ito S, #17790531).

Legends for Figures

Figure 1. Augmentation of MCh-induced contraction by S1P in ASM. A: A typical example of a simultaneous record of tension (upper trace) and F_{340}/F_{380} (lower trace) in response to 1 μM MCh before and after 3 μM S1P for 15 min. B: Concentration-response curves for S1P on tension (open circles) and F_{340}/F_{380} (closed circles). The values of percent response to S1P were expressed taking response to 1 μM MCh as 100%. C: The values of percent contraction (open columns) and F_{340}/F_{380} (closed columns) for MCh after exposure to the normal bathing solution (control) and S1P between 0.03 and 3 μM for 15 min. D: The values of percent contraction (open columns) and F_{340}/F_{380} (closed columns) for histamine after exposure to S1P in the same way in Figure 1C. E: Concentration-response curves for MCh after exposure to the normal bathing solution (open circles), 0.003 μM (closed circles) and 0.03 μM S1P (open squares) for 6 h. The abscissas in B and D express molar concentrations on a log scale. *: $p < 0.05$, **: $p < 0.01$

Figure 2. Involvement of the Rho/Rho-kinase pathway in the hyperresponsiveness to MCh induced by S1P. A: A typical example of a simultaneous record of tension (upper trace) and F_{340}/F_{380} (lower trace) in response to 1 μM MCh before and after 3 μM S1P for 15 min in the presence of 1 μM Y-27632. B: The values of percent contraction (open columns) and F_{340}/F_{380} (closed columns) for MCh after exposure to the normal bathing solution (control) and S1P in the presence of Y-27632 between 0.01 and 1.0 μM. C: Concentration-response curves for MCh after exposure to 0.03 μM S1P in the absence (open circles) and present of Y-27632 0.1 (closed circles) and 1.0 μM (open

squares) for 6 h. D: Those values of percent contraction (open columns) and F_{340}/F_{380} (closed columns) for MCh after exposure to S1P in the absence (control) and presence of 30 μM PD98059 and 10 μM bisindoylmaleimide (BIS) for an equivalent min. The abscissa in C expresses molar concentrations on a log scale. *: $p < 0.05$, **: $p < 0.01$.

Figure 3. S1P-induced airway hyperreactivity is not involved in Ca^{2+} channel activity. A: A typical example of a simultaneous record of tension (upper trace) and F_{340}/F_{380} (lower trace) in response to 1 μM MCh before and after 3 μM S1P for 15 min in the presence of 100 μM SKF96365. B: The values of percent contraction (open columns) and F_{340}/F_{380} (closed columns) for MCh after exposure to S1P in the absence (control) and presence of an equi-molar of SKF96365 and 3 μM verapamil for an equivalent time.

Figure 4. Involvement of G_i in the induction of airway hyperreactivity induced by S1P. A: A typical record of tension by 1 μM MCh before and after exposure to 3 μM S1P for 15 min subsequent to incubation with 1.0 ng/ml pertussis toxin (PTX, upper trace) and the normal bathing solution (sham, lower trace) for 6 h. B: The values of percent contraction for MCh after exposure to 3 μM S1P subsequent to incubation with the normal bathing solution (control), and an equivalent concentration of PTX for 2 – 6 h. C: Concentration-response curves for MCh after exposure to 0.03 μM S1P in the absence (open circles), and presence of 0.1 (closed circles), and 1.0 μg/ml PTX (open squares) for 6 h. The abscissa in B expresses molar concentrations on a log scale. *: $p < 0.05$, **: $p < 0.01$.

JPET Fast Forward. Published on November 14, 2006 as DOI: 10.1124/jpet.106.110718
This article has not been copyedited and formatted. The final version may differ from this version.

Figure 5. The effects of S1P on RhoA activity in the human BSM cells. Human BSM cells were incubated with the medium in the absence (control) and presence of 1 μM S1P for 15 min. Activated form of Rho (GTP-Rho) was pulled-dowm from the cell lysates with Rhotekin-binding domain-conjugated beads, and analysed by Western blotting using anti-RhoA. The identical cell lysates were used to determine total Rho. Data are representative of four independent experiments (upper trace). The value of RhoA-GTP/total RhoA by S1P is calculated relative to that for control 1 (lower trace). **: $p < 0.01$.

Figure 6. Regulation of MBS phosphorylation by S1P. Phosphorylated MBS in human BSM cells was evaluated with immunoblotting using anti-MYPT1 (Thr^{850}). A: The inhibitory effects of S1P on MBS phophorylation, B: The effects of Y-27632 on phosphorylated MBS by S1P, C: The effects of PTX and PD98059 on phosphrylated MBS by S1P. The values of p-MYPT1/MYPT1 are calculated relative to that for control at each experimental condition (open columns). *: $p < 0.05$, **: $p < 0.01$ (vs. response to control), †:$p < 0.01$ (vs. response to S1P)

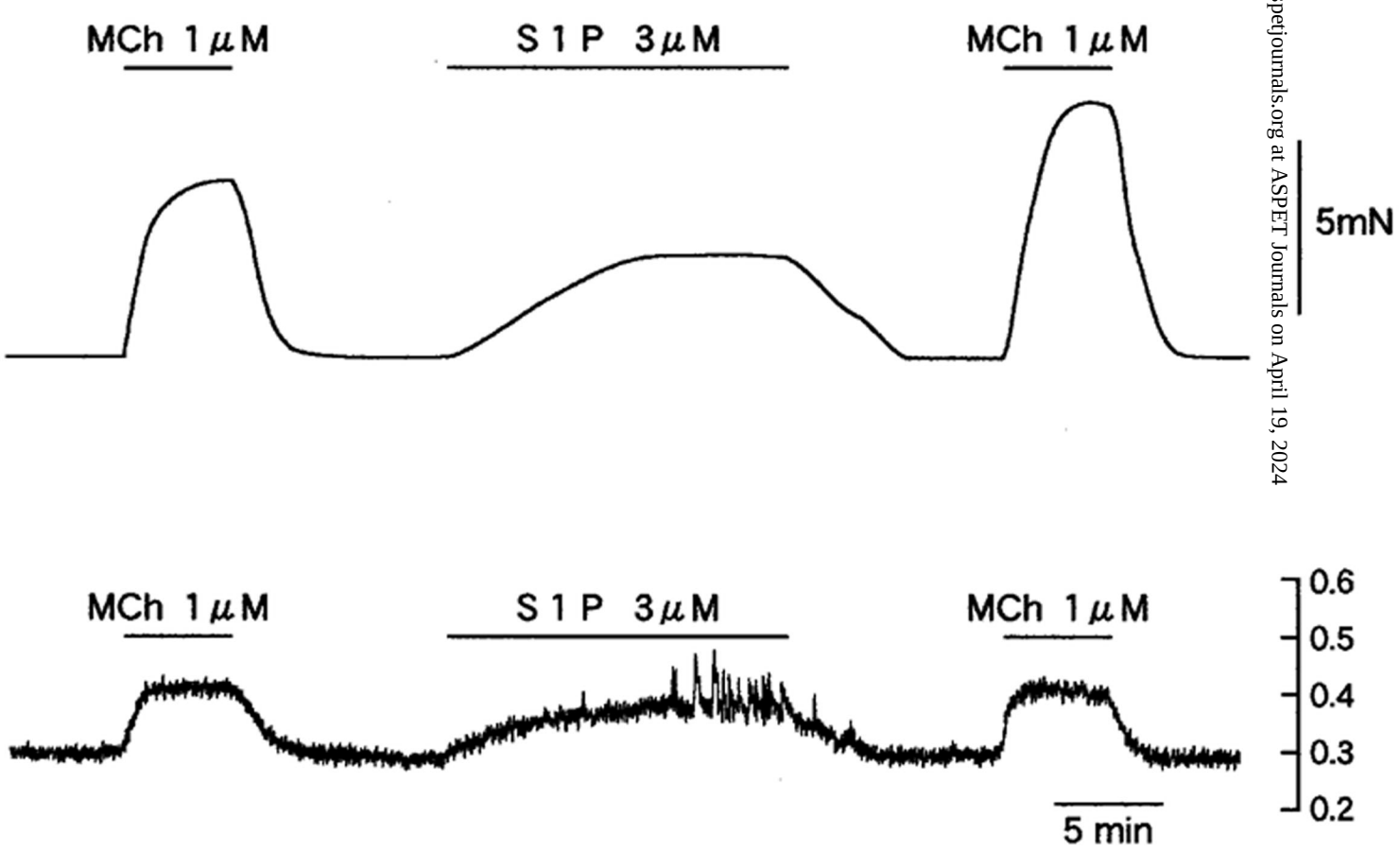

Figure 1A

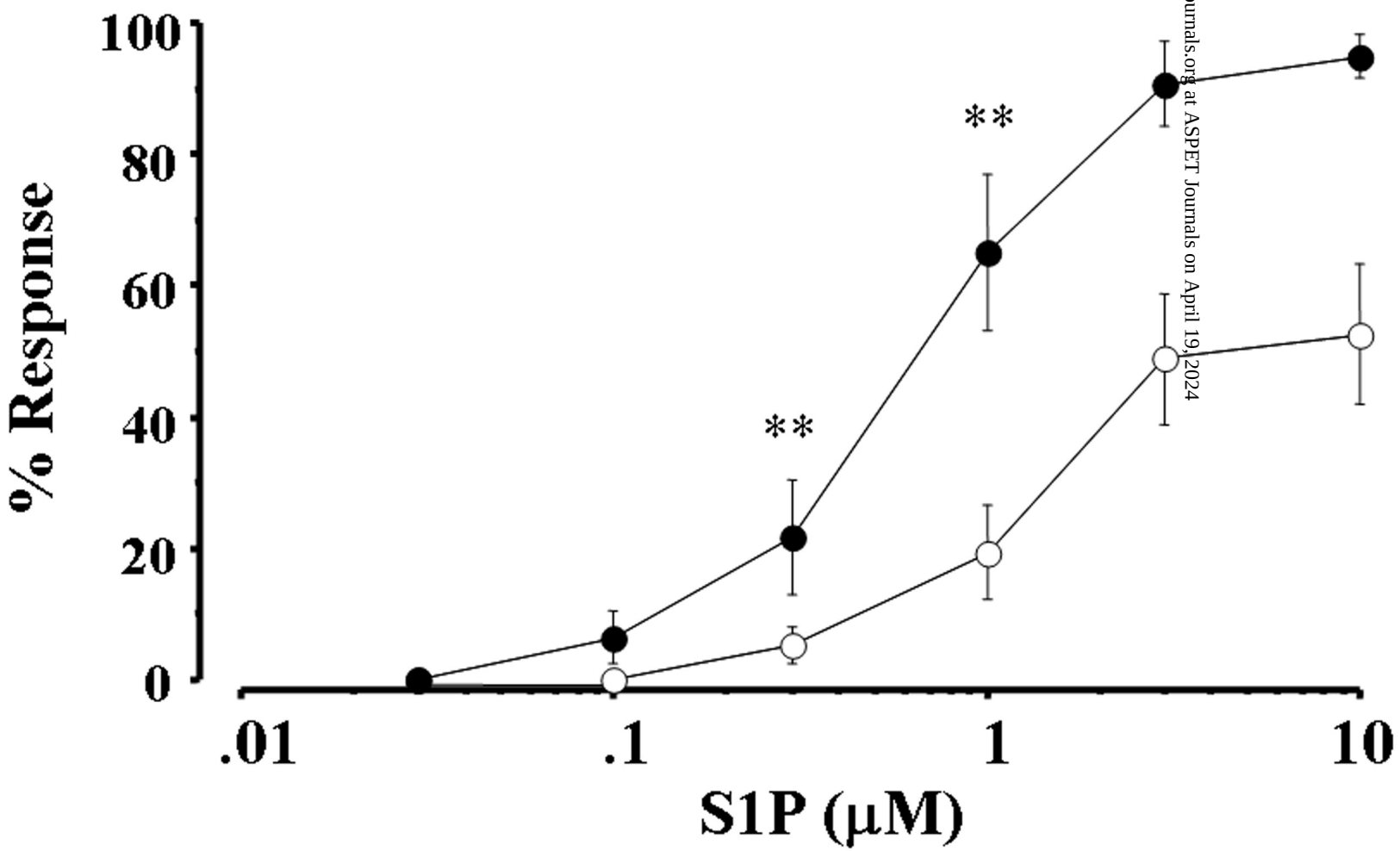

Figure 1B

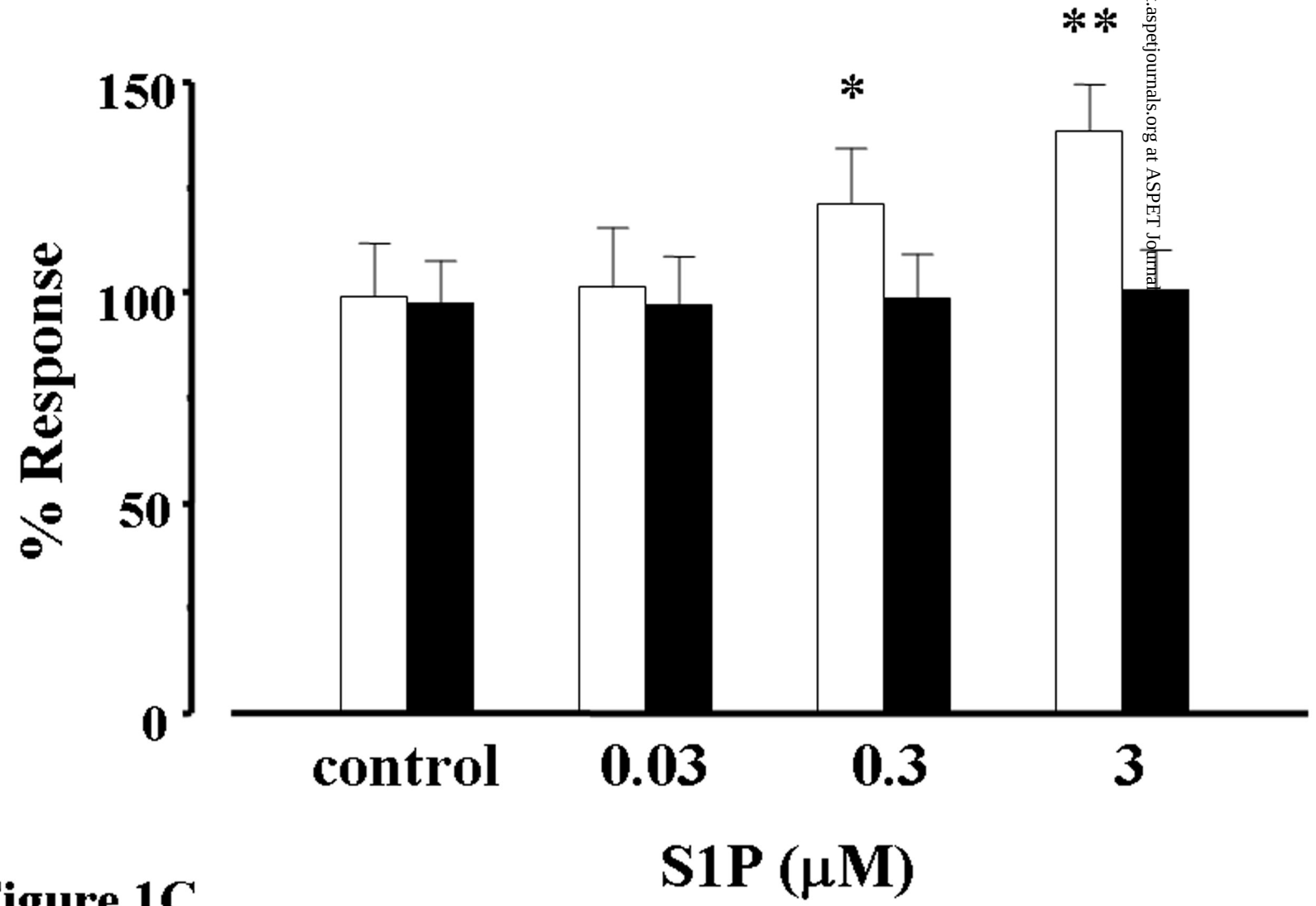

Figure 1C

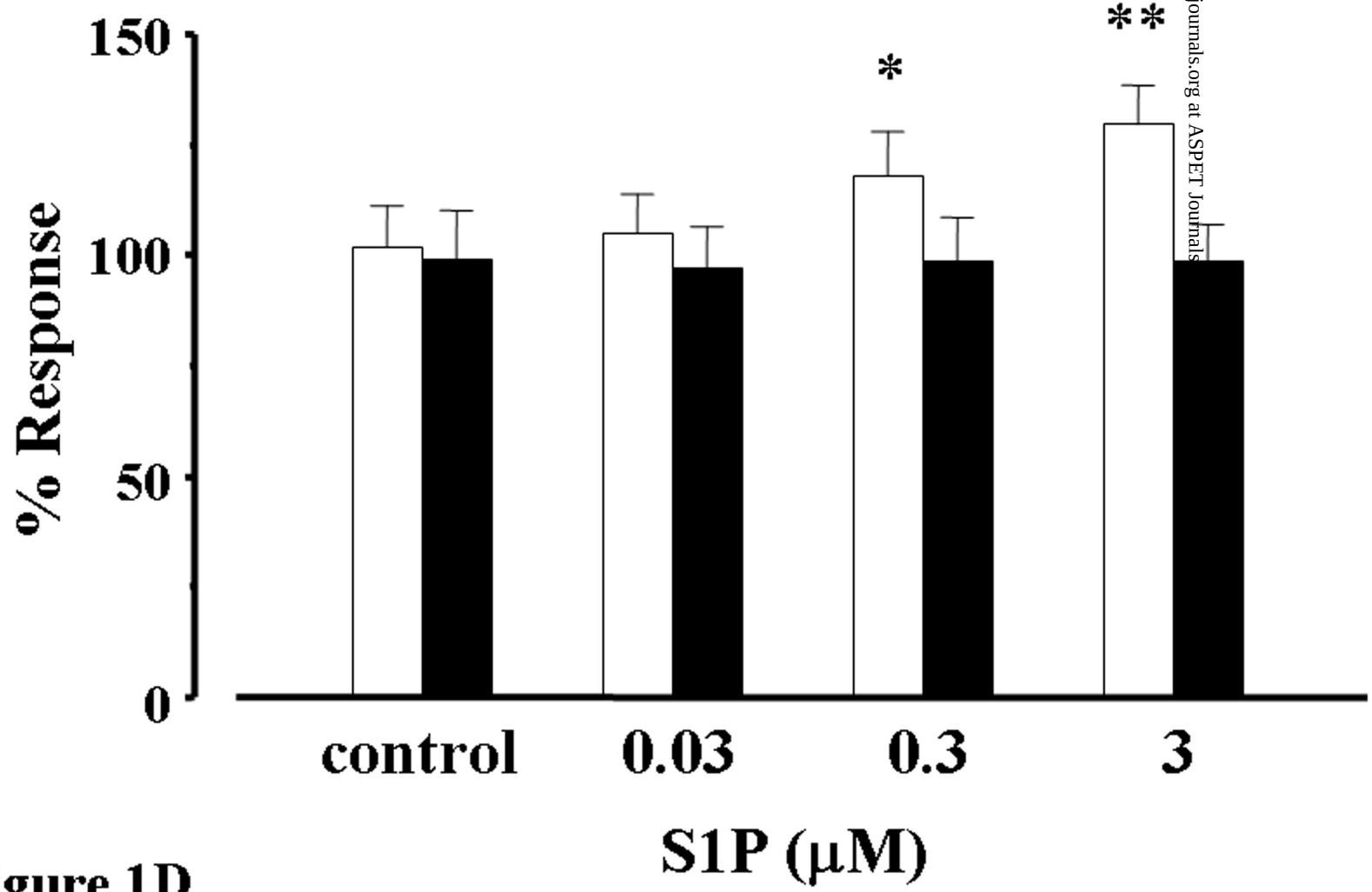

Figure 1D

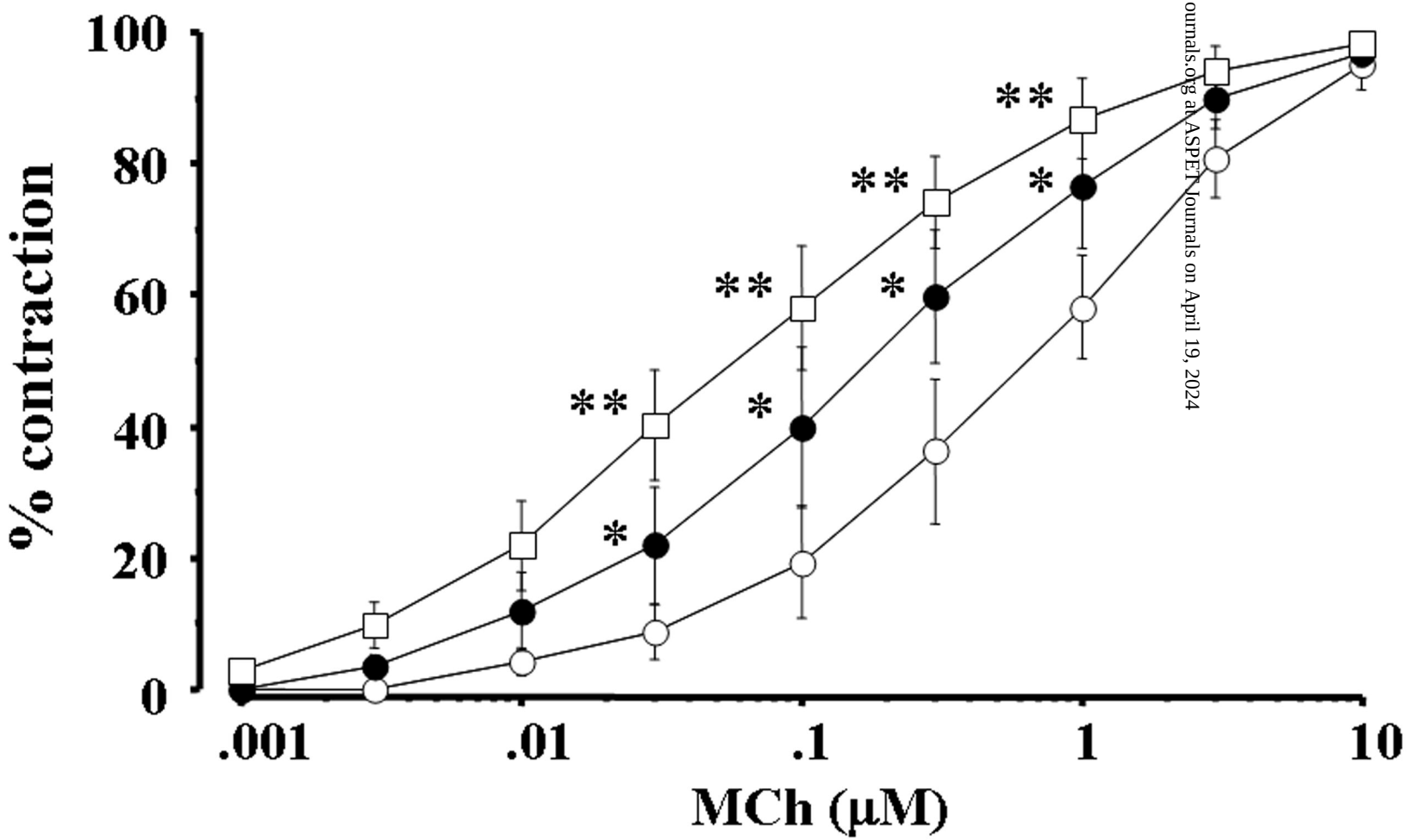

Figure 1E

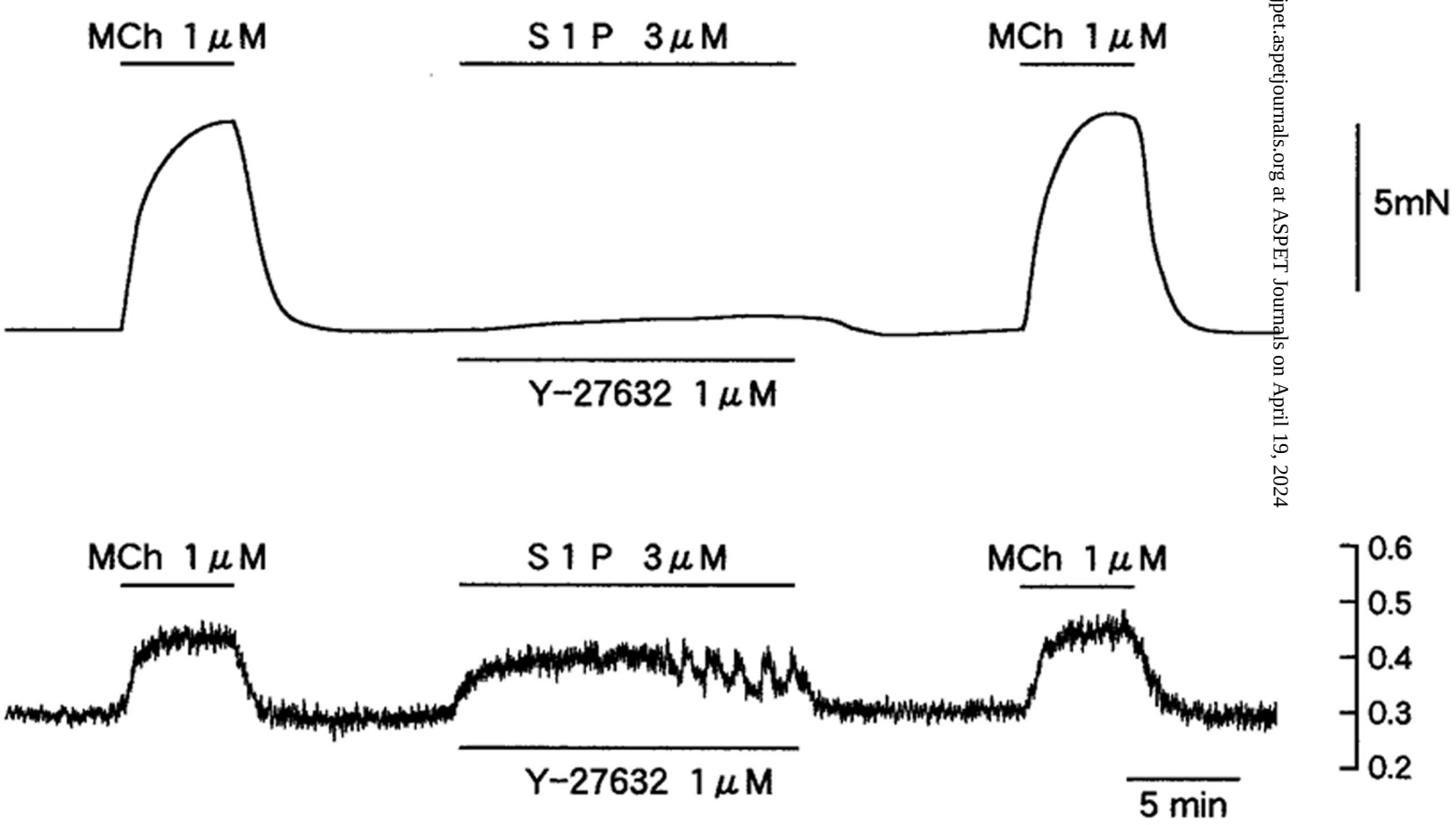

Figure 2A

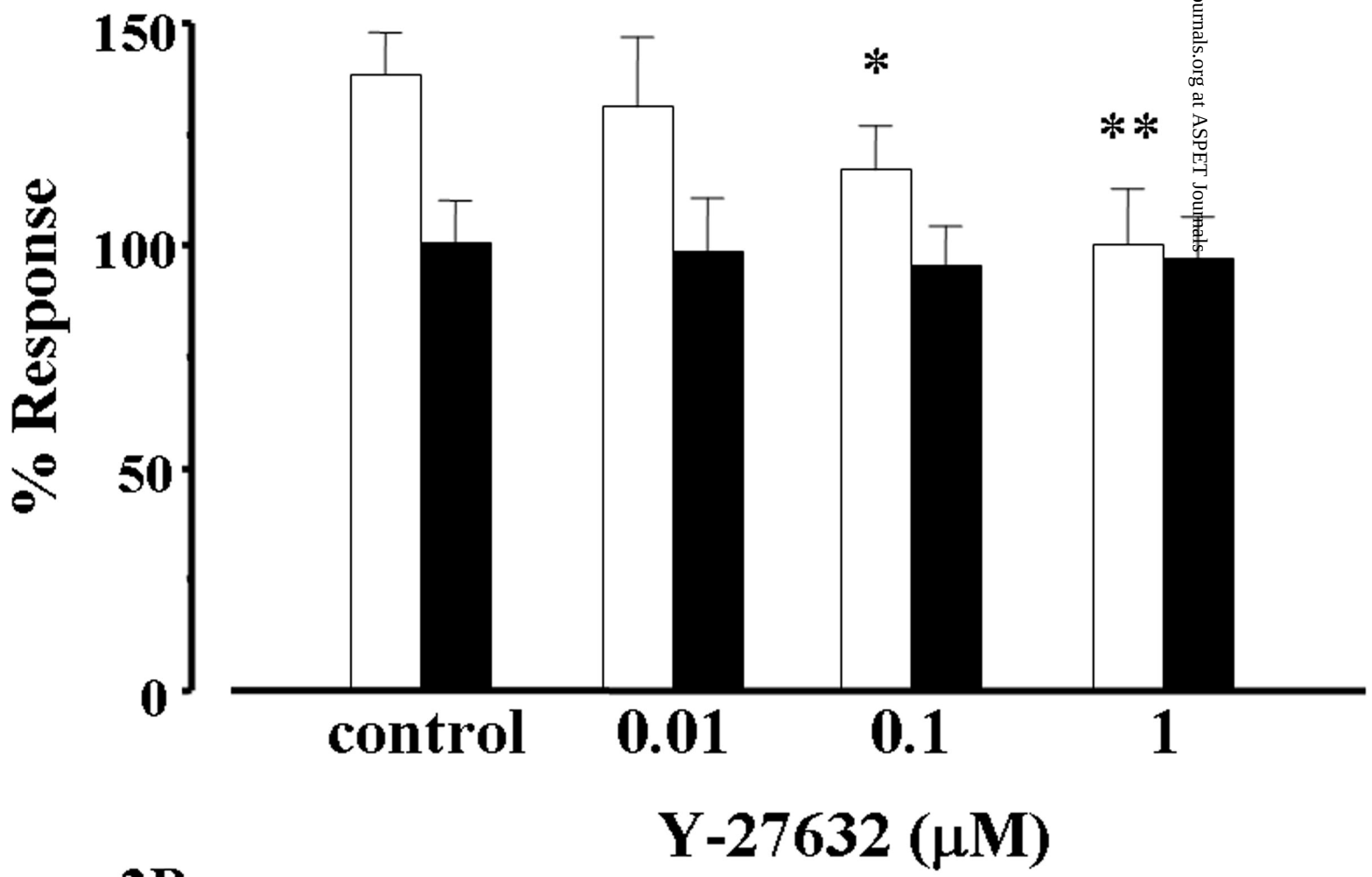

Figure 2B

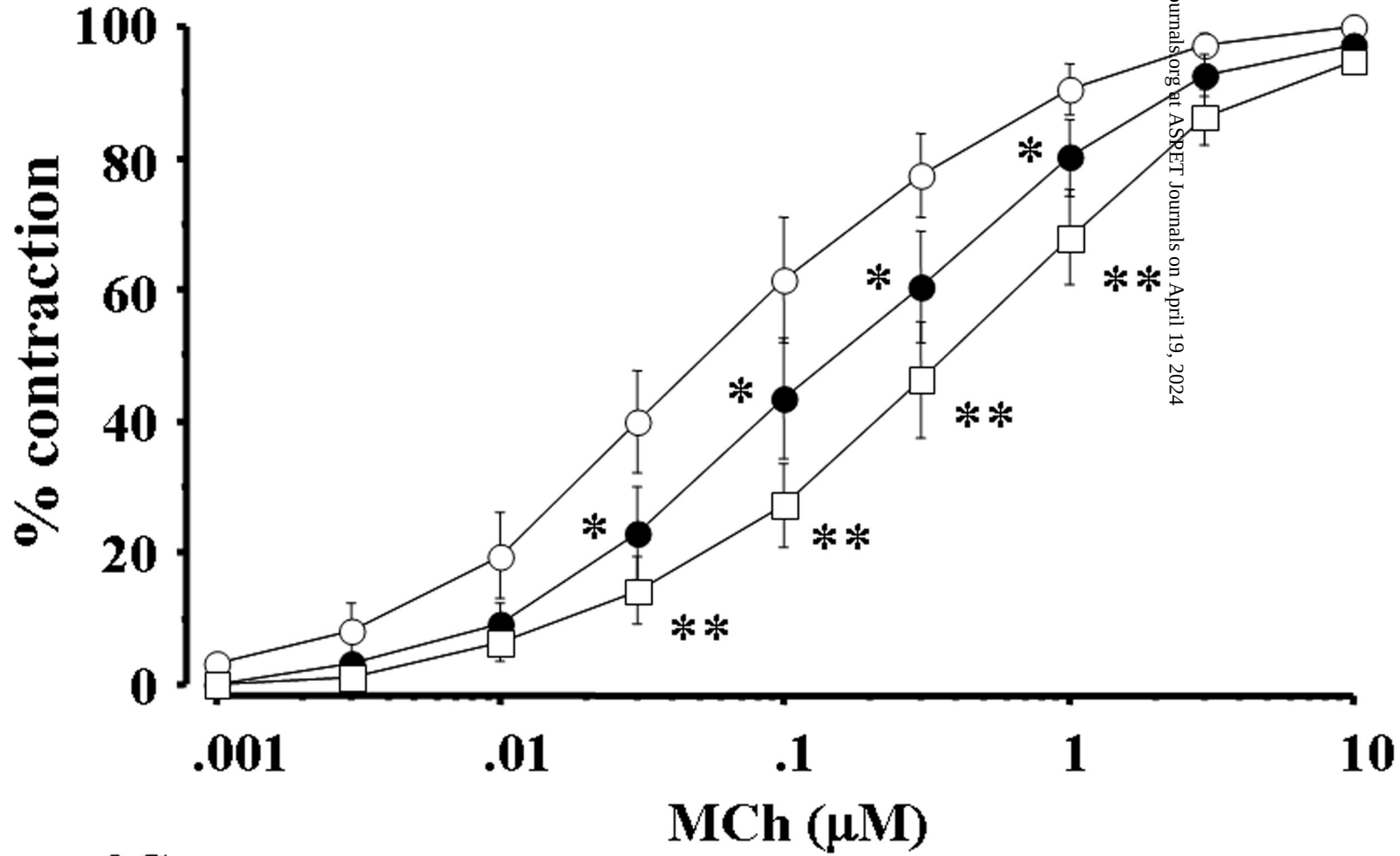

Figure 2C

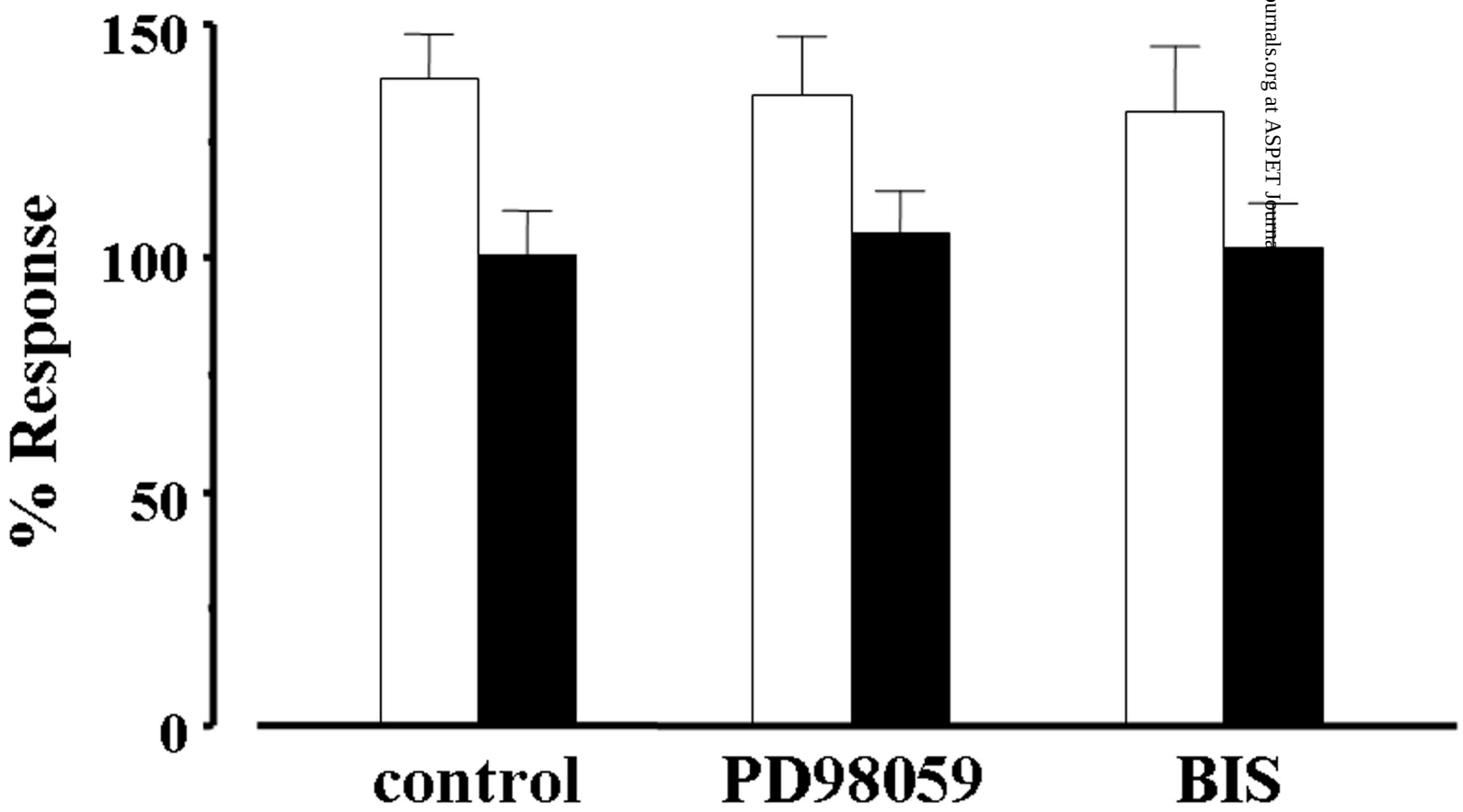

Figure 2D

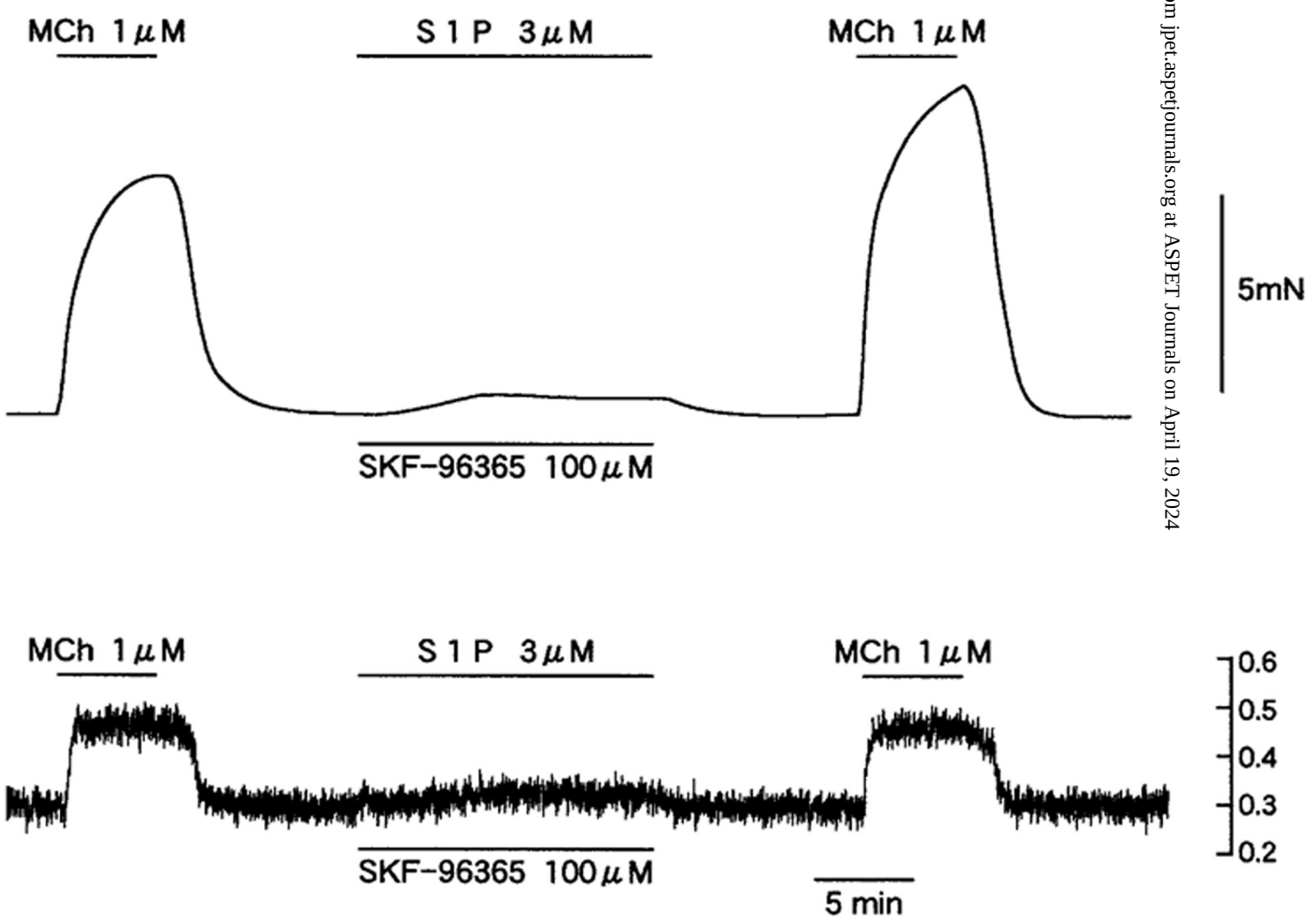

Figure 3A

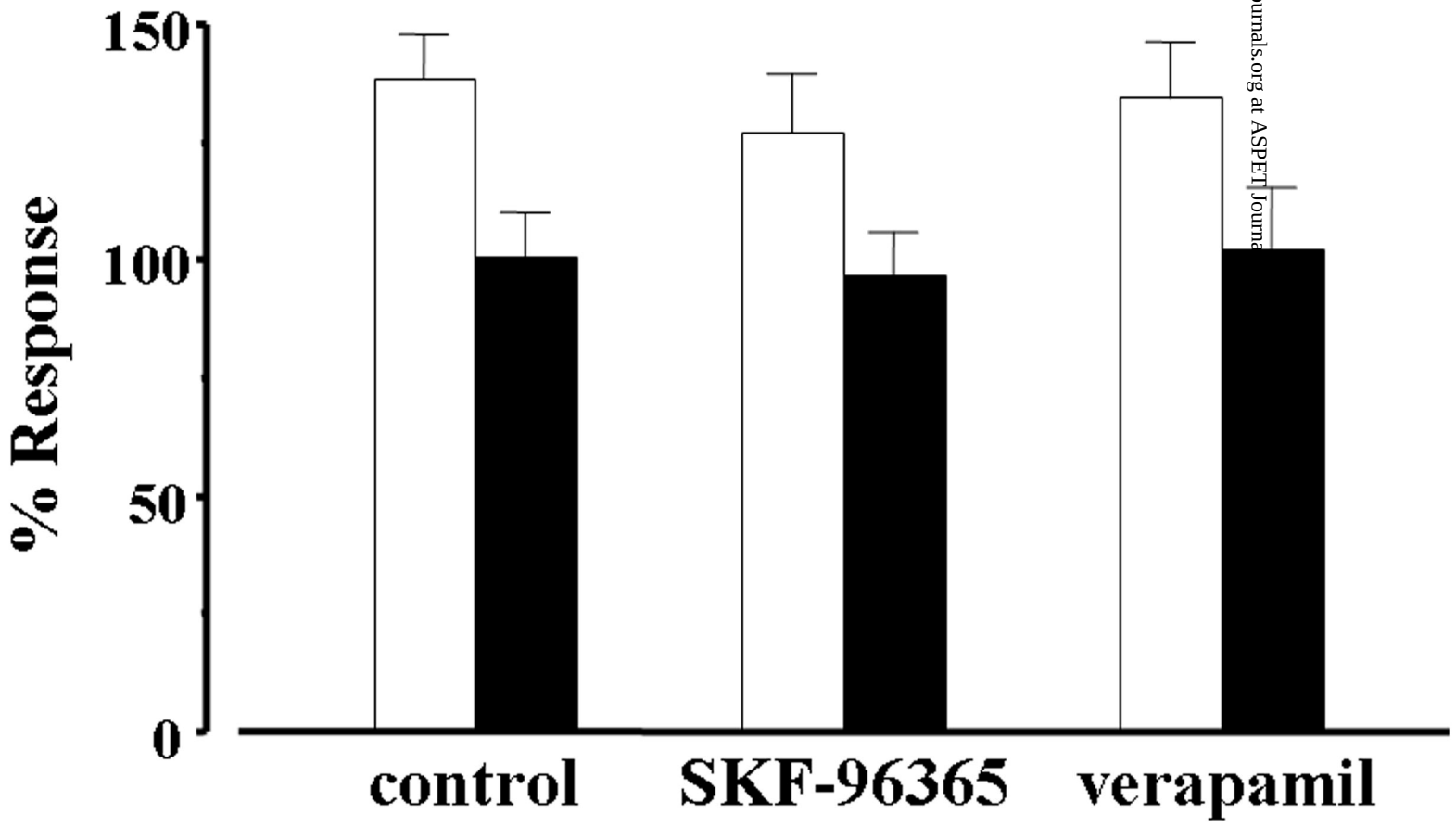

Figure 3B

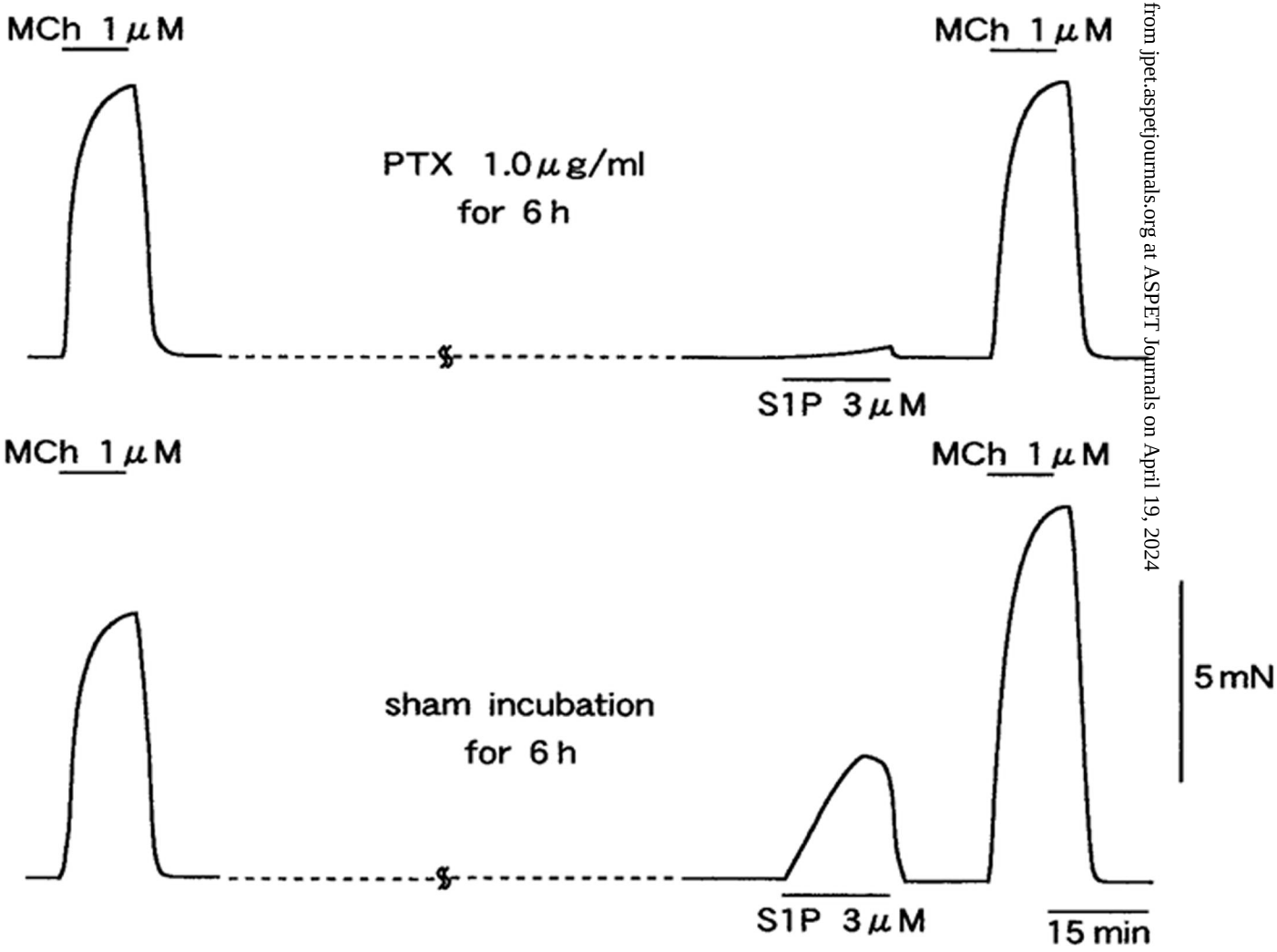

Figure 4A

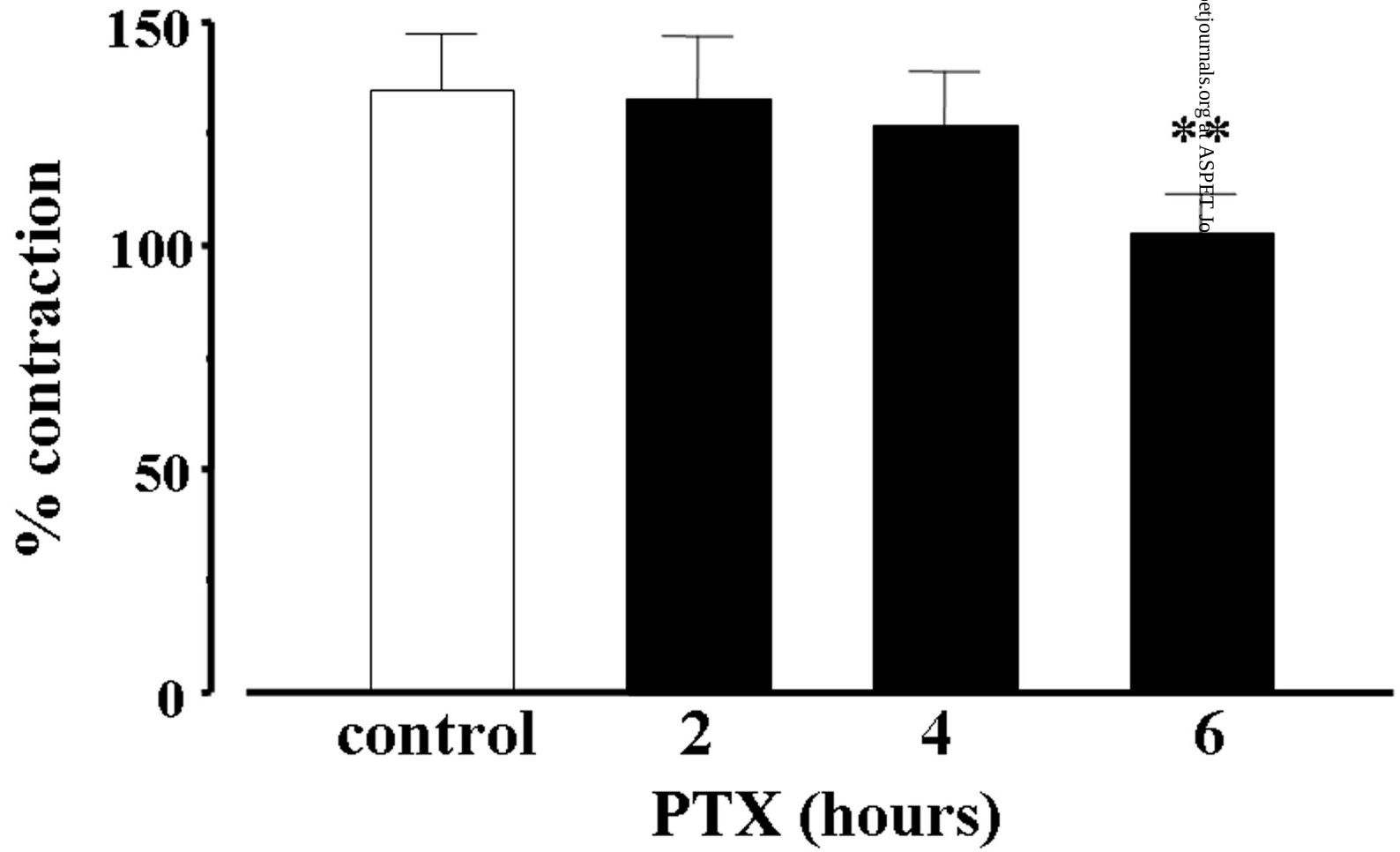

Figure 4B

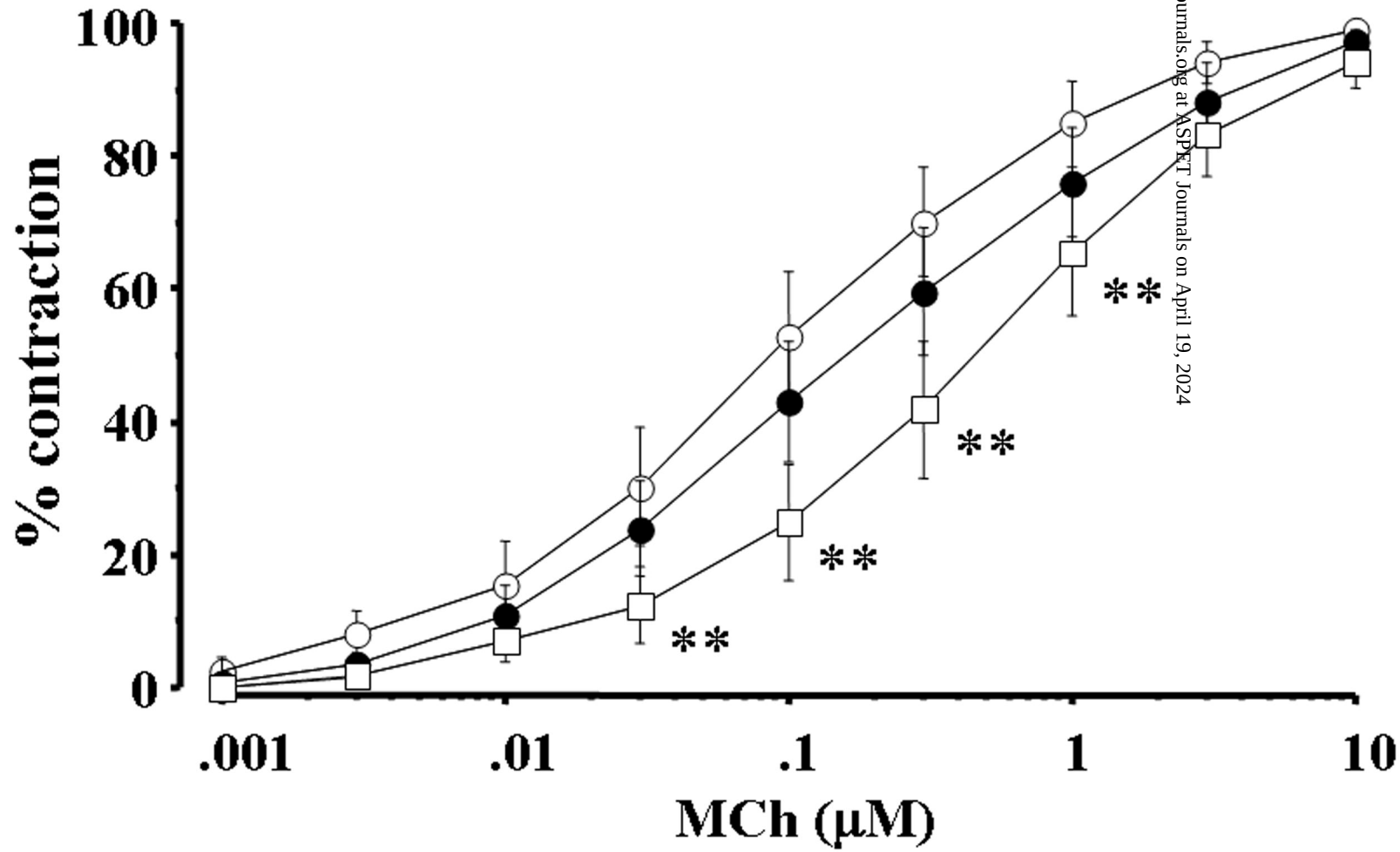

Figure 4C

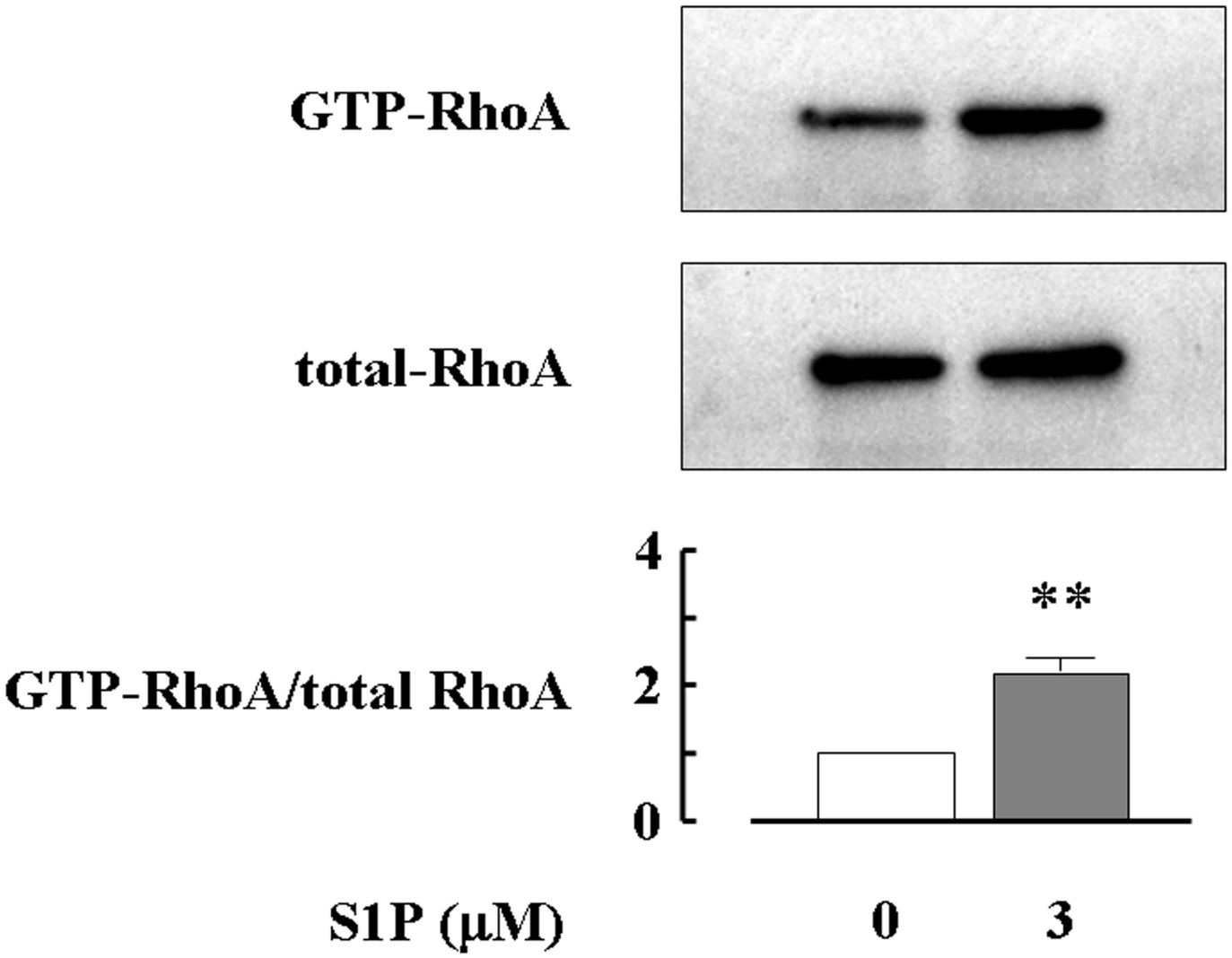

Figure 5

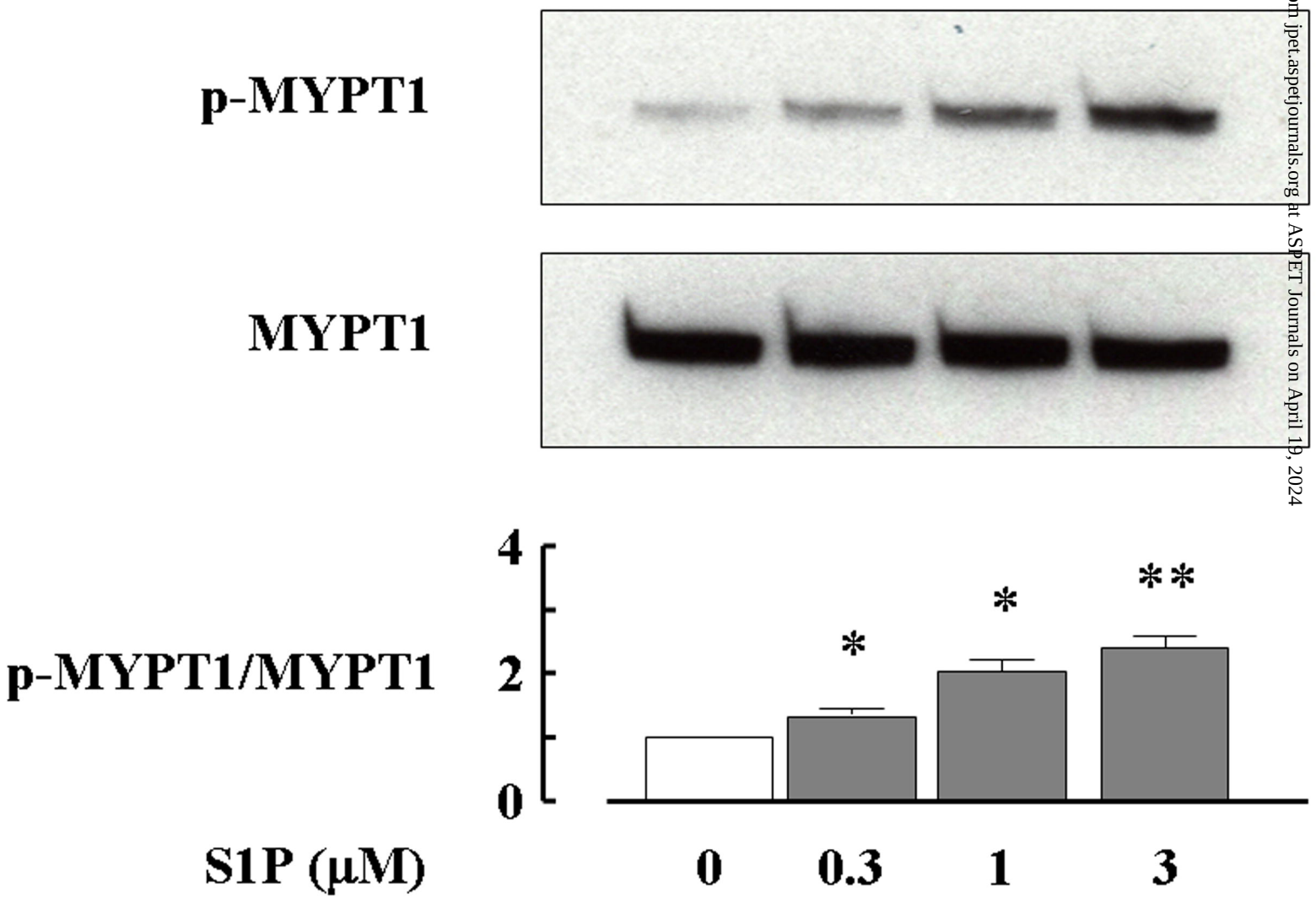

Figure 6A

Figure 6B

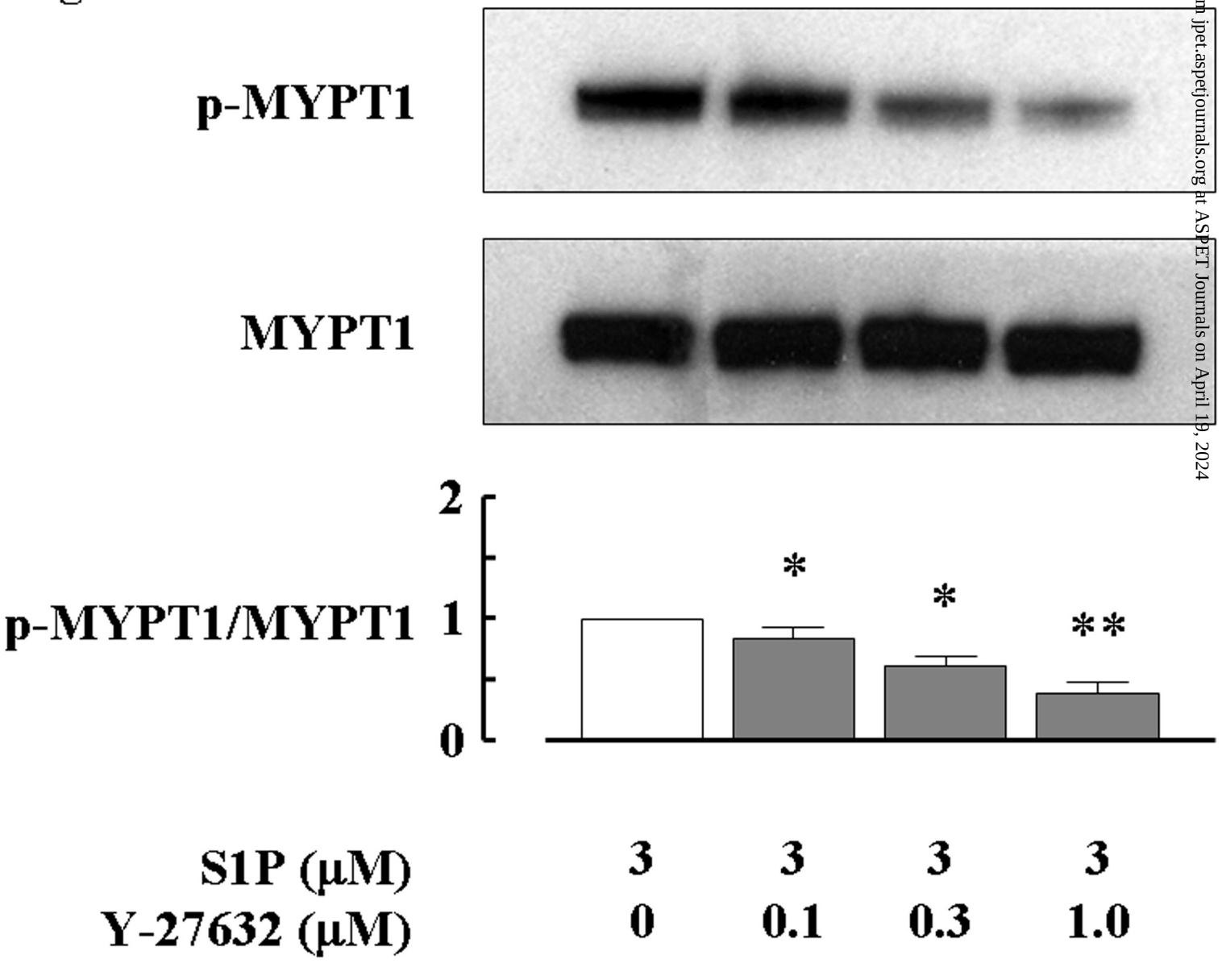

Figure 6C